

AD A 030857

SDAC-TR-76-7

FB

**THE EFFECT OF ATTENUATION  
ON THE SPECTRA OF P WAVES FROM  
NUCLEAR EXPLOSIONS IN NORTH AMERICA**

ZOLTAN A. DER AND THOMAS W. McELFRESH

Seismic Data Analysis Center

Teledyne Geotech, 314 Montgomery Street, Alexandria, Virginia 22314

1 JUNE 1976

APPROVED FOR PUBLIC RELEASE; DISTRIBUTION UNLIMITED.

Sponsored By

The Defense Advanced Research Projects Agency

Nuclear Monitoring Research Office

1400 Wilson Boulevard, Arlington, Virginia 22209

ARPA Order No. 1620

Monitored By

VELA Seismological Center

312 Montgomery Street, Alexandria, Virginia 22314

D D C  
RECEIVED  
OCT 19 1976  
UNLIMITED  
D

Disclaimer: Neither the Defense Advanced Research Projects Agency nor the Air Force Technical Applications Center will be responsible for information contained herein which has been supplied by other organizations or contractors, and this document is subject to later revision as may be necessary. The views and conclusions presented are those of the authors and should not be interpreted as necessarily representing the official policies, either expressed or implied, of the Defense Advanced Research Projects Agency, the Air Force Technical Applications Center, or the US Government.

Unclassified

SECURITY CLASSIFICATION OF THIS PAGE (When Data Entered)

REPORT DOCUMENTATION PAGE		READ INSTRUCTIONS BEFORE COMPLETING FORM	
14 1. REPORT NUMBER SDAC-TR-76-7	2. GOVT ACCESSION NO.	3. RECIPIENT'S CATALOG NUMBER	
6 4. TITLE (and Subtitle) THE EFFECT OF ATTENUATION ON THE SPECTRA OF P WAVES FROM NUCLEAR EXPLOSIONS IN NORTH AMERICA		9 5. TYPE OF REPORT & PERIOD COVERED Technical Rept.	
		6. PERFORMING ORG. REPORT NUMBER	
7. AUTHOR(s) Der, Zoltan A. and McElfresh, Thomas W.		8. CONTRACT OR GRANT NUMBER(s)	
		15 E08606-76-C-0004 WARPA Order-2557	
9. PERFORMING ORGANIZATION NAME AND ADDRESS Teledyne Geotech 314 Montgomery Street Alexandria, Virginia 22314		10. PROGRAM ELEMENT PROJECT TASK AREA & WORK UNIT NUMBERS 14 VT/6789	
11. CONTROLLING OFFICE NAME AND ADDRESS Defense Advanced Research Projects Agency Nuclear Monitoring Research Office 1400 Wilson Blvd.-Arlington, Virginia 22209		12. REPORT DATE 11 1 Jun 76	12 53p
		13. NUMBER OF PAGES 51	
14. MONITORING AGENCY NAME & ADDRESS (if different from Controlling Office) VELA Seismological Center 312 Montgomery Street Alexandria, Virginia 22314		15. SECURITY CLASS. (of this report) Unclassified	
		15a. DECLASSIFICATION DOWNGRADING SCHEDULE	
16. DISTRIBUTION STATEMENT (of this Report)  APPROVED FOR PUBLIC RELEASE; DISTRIBUTION UNLIMITED.			
17. DISTRIBUTION STATEMENT (for the abstract entered in Block 20, if different from Report) 10 Zoltan A. Der Thomas W. McElfresh			
18. SUPPLEMENTARY NOTES			
19. KEY WORDS (Continue on reverse side if necessary and identify by block number) Attenuation                      Amplitude Spectra Body Wave Magnitude          Nuclear Explosions P Wave Amplitude + star			
20. ABSTRACT (Continue on reverse side if necessary and identify by block number) Anelastic attenuation ( $t^*$ ) was measured along various paths in North America using spectra of P-waves from nuclear explosions PILEDRIVER, KNICKERBOCKER, MAST, GNOME, and SALMON to various LRSM and SDCS stations. The results are consistent with the presence of a sizeable low Q layer under the western United States (WUS) and the absence of such layer under the tectonically stable eastern part of North America. Typical values of $t^*$ at intermediate distances along paths crossing this low-Q layer are around .45. Paths outside WUS have typical $t^*$ values around .15.			

DD FORM 1 JAN 73 1473A EDITION OF 1 NOV 65 IS OBSOLETE

Unclassified  
SECURITY CLASSIFICATION OF THIS PAGE (When Data Entered)

408758

Y.P

THE EFFECT OF ATTENUATION ON THE SPECTRA OF P WAVES FROM  
NUCLEAR EXPLOSIONS IN NORTH AMERICA

SEISMIC DATA ANALYSIS CENTER REPORT NO.: SDAC-TR-76-7  
AFTAC Project Authorization No.: VELA T/6709/B/ETR  
Project Title: Seismic Data Analysis Center  
ARPA Order No.: 2551  
ARPA Program Code No.: 6F10  
Name of Contractor: TELEDYNE GEOTECH  
Contract No.: F08606-76-C-0004  
Date of Contract: 01 July 1975  
Amount of Contract: \$2,319,926  
Contract Expiration Date: 30 June 1976  
Project Manager: Royal A. Hartenberger  
(703) 836-3882

P. O. Box 334, Alexandria, Virginia 22314

APPROVED FOR PUBLIC RELEASE; DISTRIBUTION UNLIMITED.

ACCESSION for	
NTIS	White Section <input checked="" type="checkbox"/>
DDC	Buff Section <input type="checkbox"/>
UNANNOUNCED	<input type="checkbox"/>
JUSTIFICATION	
BY	
DISTRIBUTION AND AVAILABILITY CODES	
Dist	
A	

DDC  
RECEIVED  
OCT 19 1976  
D

## ABSTRACT

Anelastic attenuation ( $t^*$ ) was measured along various paths in North America using spectra of P-waves from nuclear explosions PILEDRIVER, KNICKERBOCKER, MAST, GNOME, and SALMON to various LRSM and SDCS stations. The results are consistent with the presence of a sizeable low Q layer under the western United States (WUS) and the absence of such layer under the tectonically stable eastern part of North America. Typical values of  $t^*$  at intermediate distances along paths crossing this low-Q layer are around .45. Paths outside WUS have typical  $t^*$  values around .15.

## TABLE OF CONTENTS

	Page
ABSTRACT	2
INTRODUCTION	7
DATA ANALYSIS	9
<u>PILEDRIVER</u>	9
<u>KNICKERBOCKER</u>	13
<u>MAST</u>	19
<u>GNOME</u>	19
<u>SALMON</u>	33
DISCUSSION	42
ACKNOWLEDGEMENTS	48
REFERENCES	49
APPENDIX - Procedures Followed in Computing Q	50

## LIST OF FIGURES

Figure No.	Title	Page
1	Particle velocity waveform of PILEDRIVER 1543 feet horizontally from the shot point.	11
2	Source displacement spectra for PILEDRIVER. Solid line - derived from particle velocity waveform. Dashed line - upscaled granite source spectrum.	12
3	P-wave traces from PILEDRIVER.	14
4	P-wave power spectra from PILEDRIVER 9(not corrected for instrument response).	15
5	P-wave to source spectral ratios with straight line fits for PILEDRIVER.	16
6	Location of PILEDRIVER and the recording stations with $t^*$ values derived from data.	18
7	Source spectrum used for analysis of KNICKERBOCKER data.	20
8	P-wave traces from KNICKERBOCKER.	21
9	P-wave power spectra from KNICKERBOCKER.	22
10	P-wave to source spectral ratios for KNICKERBOCKER.	23
11	Location of KNICKERBOCKER and the recording stations with $t^*$ values.	24
12	MAST reduced displacement potential scaled to 20 tons.	26
13	MAST source spectrum used in our analysis (solid line) and upscaled source spectrum of von Seggern and Blandford (1972).	27
14	P-wave traces for MAST.	28
15	P-wave power spectra for MAST.	29
16	P-wave to source spectral ratios for MAST.	30

LIST OF FIGURES (Continued)

Figure No.	Title	Page
17	Location of MAST and the recording stations with $t^*$ values.	31
18	GNOME source spectrum.	34
19	P-wave traces for GNOME.	35
20	P-wave power spectra for GNOME.	36
21	P-wave to source spectral ratios for GNOME.	37
22	Location of GNOME and the recording stations with $t^*$ values.	38
23	Location of SALMON and the recording stations with $t^*$ values.	40
24	Histograms of all $t^*$ measurements quoted in this paper.	45
25	Plots of $\log A/T$ ( $m\mu/\text{sec}$ ) vs. $t^*$ for GNOME and SALMON. Distance (B factor) corrections have been made on $\log (A/T)$ .	46



LIST OF TABLES

Table No.	Title	Page
I	Relevant Data for the Nuclear Explosions used in this study.	10
II	Summary of the Results of Attenuation Calculations	17
IIA	PILED RIVER	17
IIB	KNICKERBOCKER	25
IIC	MAST	32
IID	GNOME	39
IIE	SALMON	41

## INTRODUCTION

This study is a continuation of previous work aimed at defining regional attenuation patterns for short-period P-waves in North America (Der and McElfresh, 1975). In this work we use several NTS explosions in hard rock (granite or rhyolite) and the nuclear explosion GNOME which, like SALMON, was exploded in salt. The basic methods of analysis were outlined in our report on SALMON and are summarized briefly in the Appendix. Source spectra were derived from close-in measurements when such data were available; in one case (KNICKERBOCKER) we scaled the spectrum of an explosion in granite up to the yield of the explosion. We consider the direct determination of spectrum from close-in measurements more reliable. One naturally expects that by the principle of seismic reciprocity wavepaths will show the same attenuation when the wave travels either in the forward or the reverse direction. This will also be true for wavepaths which, although not exactly reciprocal, are subdivided in a similar way between high Q and low Q portions no matter in which direction the wave travels. Low Q for body waves seem to be the property of the upper mantle in Western United States (WUS) while in the eastern United States (EUS) Q remains high. It may be expected, therefore, that wavepaths which consists of approximately equal portions in the WUS and EUS respectively will show similar Q values. The possibility must be considered however when interpreting the results that there may be in either major region small subregions where the upper mantle Q differs considerably from the wide regional value. An occasional anomalous Q measurement may also be caused by other factors not properly corrected for in our procedure. In our experience such instances are rare and in general most of our results can easily be reconciled with the notion of the WUS being underlain with a low Q

---

Der, Z. A. and T. W. McElfresh, 1975, Short-period P-wave attenuation along various paths in North America as determined from P-wave spectra of the SALMON nuclear explosion, SDAC-TR-75-16, Teledyne Geotech, Alexandria, Virginia.

layer in the upper mantle which is fairly homogeneous horizontally and an EUS where such a layer is uniformly absent and the Q which remains high to great depths. The knowledge of Q values is needed to correct the observed spectra for anelastic attenuation and evaluate short-period P wave spectral discriminants.

## DATA ANALYSIS

In our analysis we have used three NTS explosions (PILEDRIVER, KNICKERBOCKER, and MAST) and GNOME, an explosion in New Mexico. NTS is deep inside the Western United States while GNOME was situated close to the boundary of the EUS as defined in the geophysical sense (Booth, Marshall and Young, 1975; Der, Massé and Gurski, 1975). We shall discuss each event separately.

### PILEDRIVER

PILEDRIVER, a 56 kt explosion in granite, was instrumented at close range and we have used the close-in velocity time history to derive a source spectrum for this event. The velocity time history is shown in Figure 1. We Fourier transformed this waveform and derived the far-field spectrum in the frequency domain by multiplying or dividing with the proper  $\omega$  factors and solving the algebraic equations for the Fourier transform of the reduced displacement potential. These operations replace the equivalent differentiation and integrations in the time domain. We have also computed the scaled far-field displacement spectrum using the source model of von Seggern and Blandford (1972). Both spectra are shown in Figure 2. There seems to be a considerable difference between the two spectra, which indicates that scaling relationships are not strictly valid. The scaled spectrum has a lower corner frequency, but the fall-off rate of the two spectra at the high frequency end is about the same. The first impression from this figure is that scaling is doubtful as a means of determining source spectra in various kinds of hard rock. This may be true as far as determining exact corner frequencies and fall-off rates is concerned. We must point out, however, that for our work we can

---

Booth, D. C., P. D. Marshall, and J. B. Young, 1975, Long and short period amplitudes from earthquakes in the range  $0^{\circ}$ - $114^{\circ}$ , *Geophys. J. R. Astr. Soc.*, v. 39, p. 523-538.

Der, Z. A., R. P. Massé, and J. P. Gurski, 1975, Regional attenuation of short-period P and S waves in the United States, *Geophys. J. R. Astr. Soc.*, v. 40, p. 85-106.

von Seggern, D. H. and R. R. Blandford, 1972, Source-time functions and spectra for underground nuclear explosions, *Geophys. J. R. Astr. Soc.*, v. 31, p. 83-97.

TABLE I

Relevant Data for the Nuclear Explosions used in this study

NAME	DATE	TIME Z	LAT	LOCATION	LONG	DEPTH ft	YIELD kt	MAG
SALMON	22 Oct 64	16:00:00.0	31° 8' 31.57" N	89° 34' 11.78" W	2717	5	4.6	
PILED RIVER	2 Jun 66	15:30:00.1	37° 13' 37.00" N	116° 3' 20.00" W	1518	55	5.5	
KNICKERBOCKER	26 May 67	15:00:00.0	37° 14' 53.00" N	116° 28' 49.00" W	2080	71	5.5	
GNOME	10 Dec 61	19:00:00.1	32° 15' 50.00" N	103° 51' 57.00" W	1200	3	4.6	
MAST	19 Jun 75	13:00:01.0	37° 18' 00.00" N	116° 18' 00.00" W			5.9	

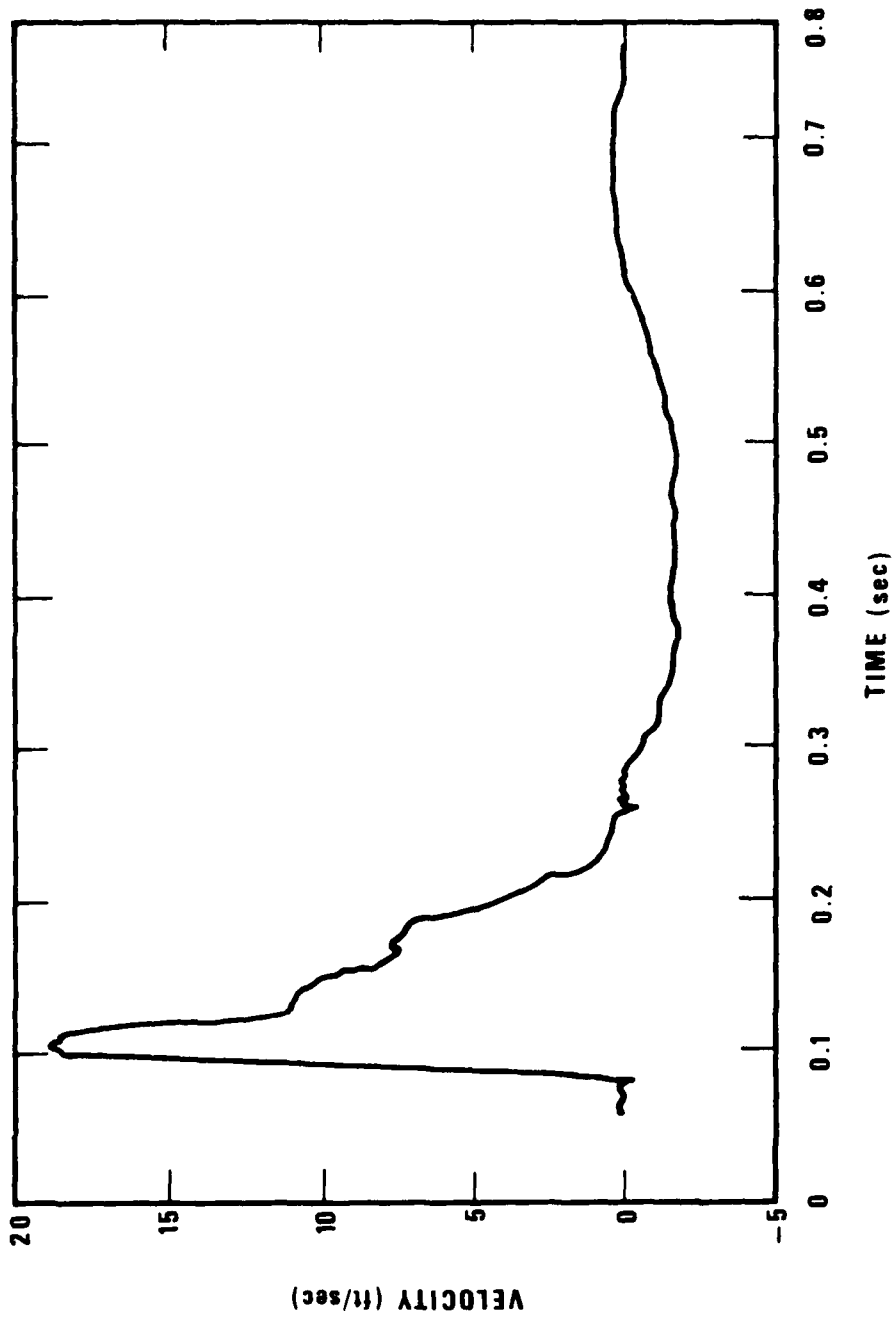


Figure 1. Particle velocity waveform of PILED RIVER 1543 feet horizontally from the shot point.

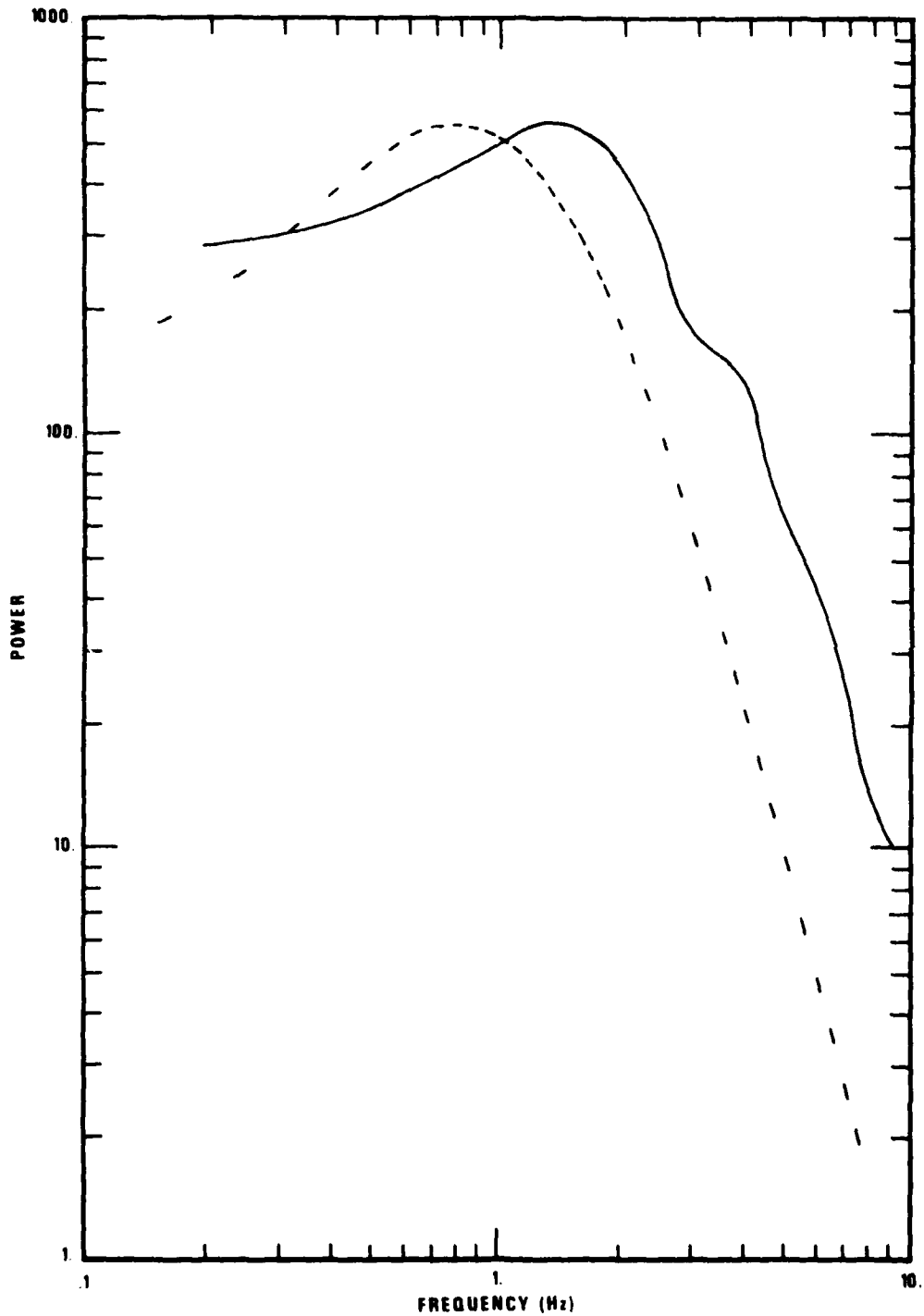


Figure 2. Source displacement spectra for PILED RIVER. Solid line - derived from particle velocity waveform. Dashed line - upscaled granite source spectrum.

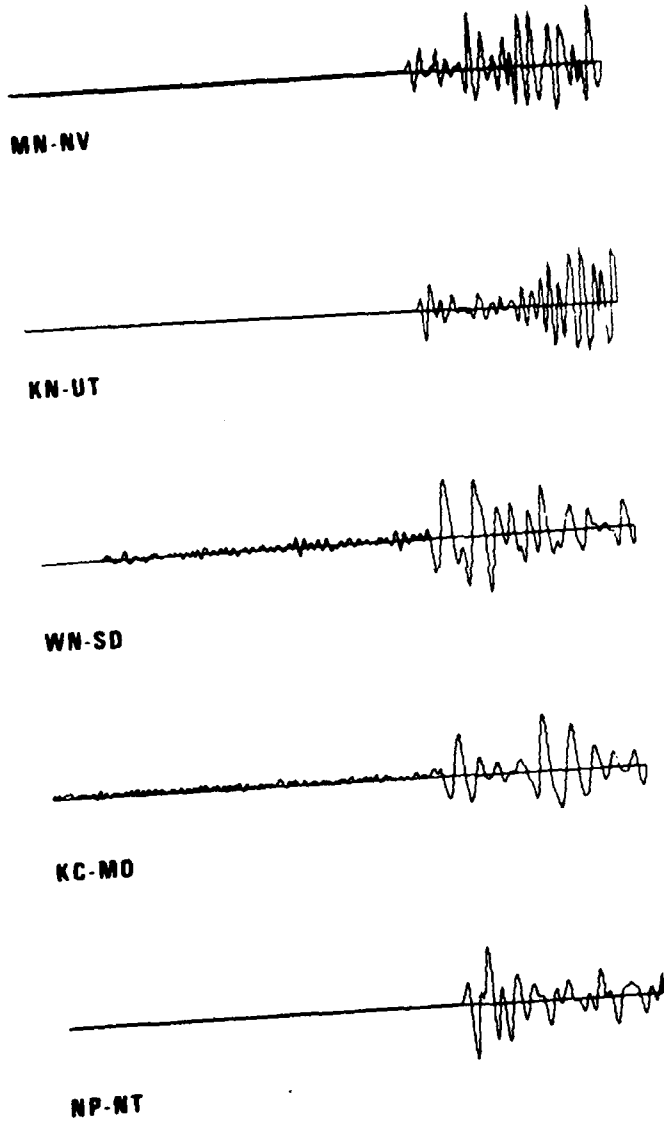
use spectra which are quite crude. First of all, what really matters in the estimation of  $Q$  or  $t^*$  is the general slope that can be fitted to the two spectra in the frequency interval .5-4. Hz, which is not very different for the two spectra. (Amplitude is proportional to  $\exp(-\omega T/2Q) = \exp(-\omega t^*/2)$  where  $T$  is the travel time.) The variation of these slopes is much less than the difference between extremes of far-field spectral slopes attributable to different degrees of attenuation (Der and McElfresh, 1975). In Figure 2 the two spectra were plotted such that the peak values were on the same level. Since we use spectral ratios the absolute magnitude of spectra is irrelevant, and if the spectra are shifted up and down on the logarithmic scale, the similarity in slopes can be better seen. The uncertainties of source spectra will influence the close-in ( $\Delta < 1000$  km)  $Q$  values considerably, but at greater distances the  $Q$  values depend very little on which spectrum is used. We have used the spectrum directly derived from the velocity time history to derive our  $Q$  values. Scaled spectra gave  $Q$ 's which were not too different from those presented in this report, except at the two close-in stations (MNV and KNUT). Figure 3 shows all the time traces used in the analysis of PILEDRIVER data. The traces at teleseismic distances reveal the effect of attenuation by their lower dominant frequency. The P-wave power spectrum and the ratios of these spectra to the source spectrum are given in Figures 4 and 5. The results of attenuation calculations are summarized in Table II. Figure 6 shows the location of the shot and all the LRSM stations used and the  $t^*$  values obtained for the paths from this explosion to each station.

#### KNICKERBOCKER

This event was recorded at a larger number of LRSM stations, but we do not have close-in measurement data for it. Its yield was 71 kilotons. We used a scaled source spectra in this case. As we pointed it out above this spectrum may differ for the actual spectrum but the  $Q$  values derived from it will be approximately correct, since at teleseismic distances the spectral slope due to attenuation has a much greater influence on the spectral ratio than any moderate uncertainties in the source spectra. The granite explosion source spectrum of von Seggern and Blandford (1972) scaled to the yield of



# PILEDRIVER



5 SEC

Figure 3. P-wave traces from PILEDRIVER.

# PILEDRIIVER

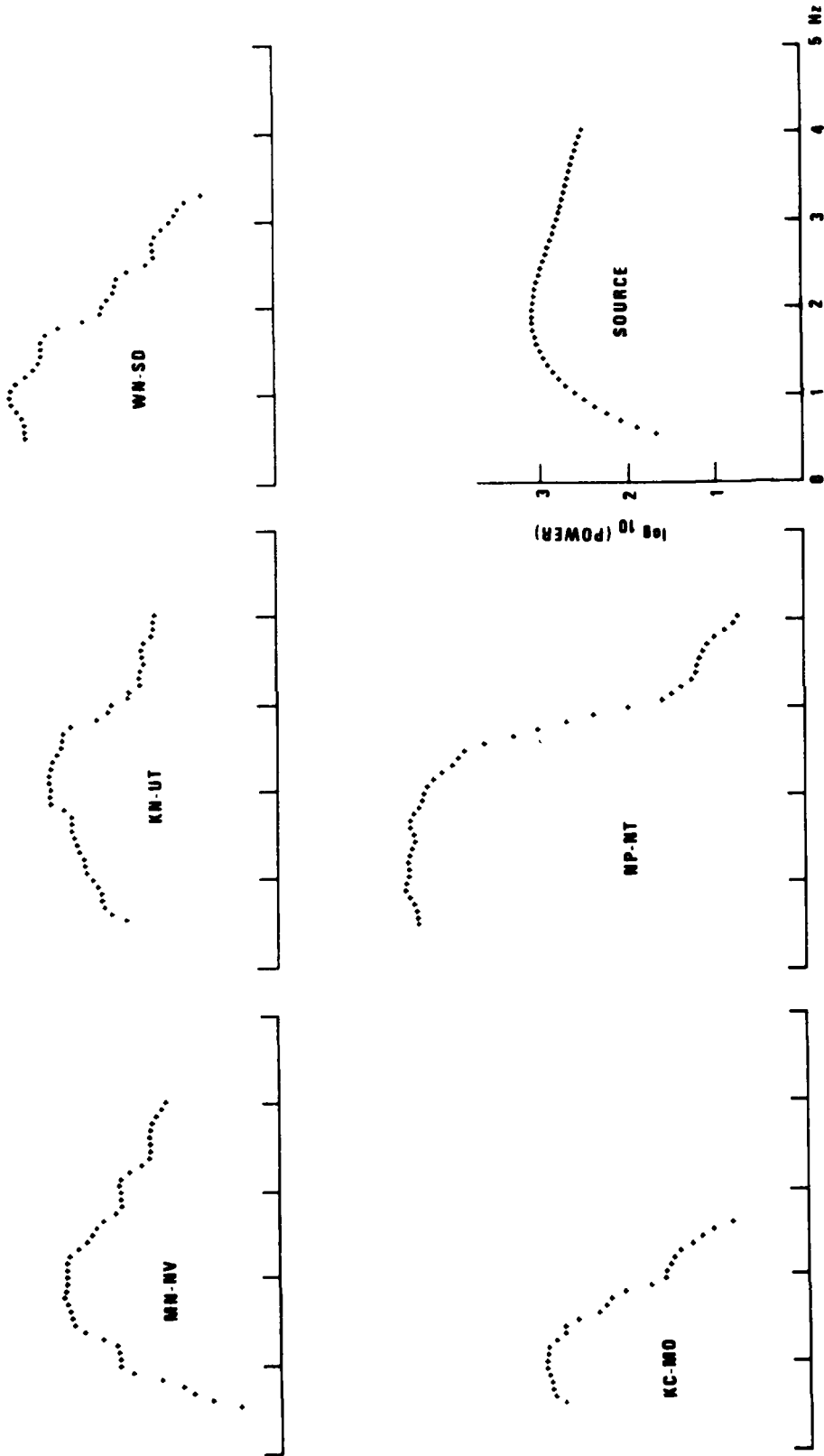
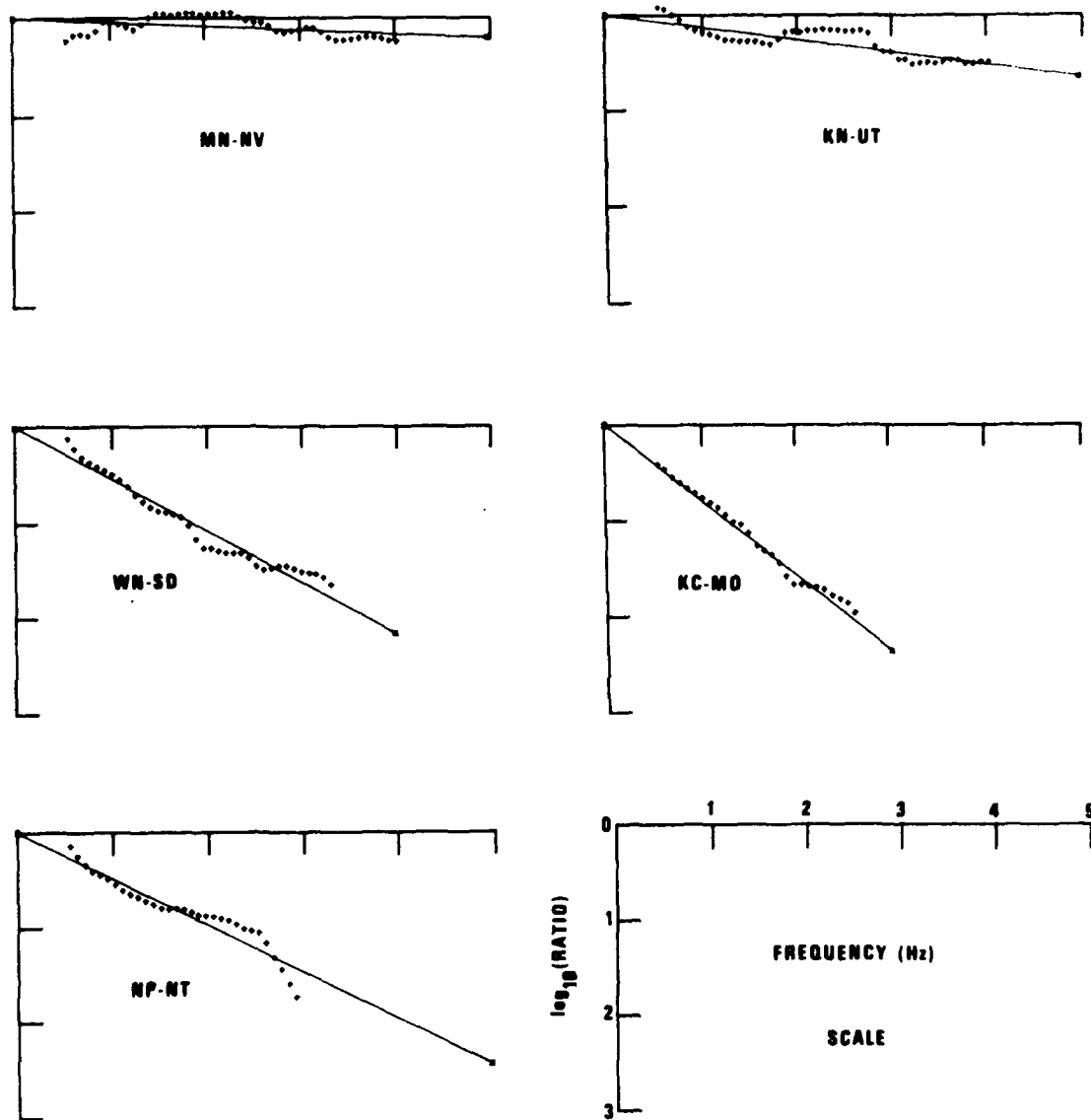


Figure 4. P-wave power spectra from PILEDRIIVER (not corrected for instrument response).

# PILEDRIVER



Ratios of Log Power Spectra of PILED RIVER to Source Spectrum derived directly from Velocity

Figure 5. P-wave to source spectral ratios with straight line fits for PILED RIVER.

TABLE II  
 Summary of the Results of Attenuation Calculations  
 TABLE IIA  
 PILED RIVER  
 58 kt

Station	Distance km	T Travel Time sec	$\alpha$ Slope	Q	$t^*$
MN-NV	228	36.3	-0.042	1179	.031
KN-UT	288	44.1	-0.141	427	.103
WN-SD	1503	195.6	-0.544	491	.398
KC-MO	1882	239.7	-0.810	404	.593
NP-NT	4353	450.6	-0.492	1250	.360



Figure 6. Location of PILEDRIVER and the recording stations with  $t^*$  values derived from data.

KNICKERBOCKER is shown in Figure 7. The time traces used are shown in Figure 8, the spectra and spectral ratios in Figures 9 and 10. A map showing the locations of the shot and the stations used is shown in Figure 11. The calculation results are summarized in Table IIB.

#### MAST

This shot was fired in rhyolite at NTS. A reduced displacement potential time trace was available (Cherry et al., 1975) which was scaled to the yield of 20 tons (Figure 12). We scaled this time function to an approximate yield of MAST which we estimated from surface wave magnitudes given in the SDCS reports. Such yield determination is very crude, but is sufficient since uncertainties about the accuracy of scaling relationships are more serious. Going through the usual procedure we derived a source spectrum which is shown in Figure 13. To check this spectrum we also scaled the spectrum of von Seggern and Blandford (1972) for the same yield. This is also shown in the same figure. The agreement between the two spectra is only fair. We used the spectrum derived from the RDP in our calculations. Again, very similar results can be obtained by using the scaled spectrum, the discussion about the spectra above applies in this case, too. The time traces, spectra and the spectral ratios are given in Figures 14, 15 and 16. The map of the shot, station locations and  $t^*$  values is shown in Figure 17, computational results are summarized in Table IIC.

#### GNOME

This 3 kt shot in a salt dome in New Mexico was widely recorded throughout the United States. The shot location is close to the boundary of the western and eastern United States as defined by sudden changes of many geophysical parameters across this boundary (Booth, Marshall and Young, 1975; Der, Massé and Gurski, 1975). The source spectrum we used was taken from an

---

Cherry, J. T., N. Rimer, J. M. Savino, and W. O. Wray, 1975, Improved yield determination and event identification research, Systems, Science and Software, SSS-R-75-2696.

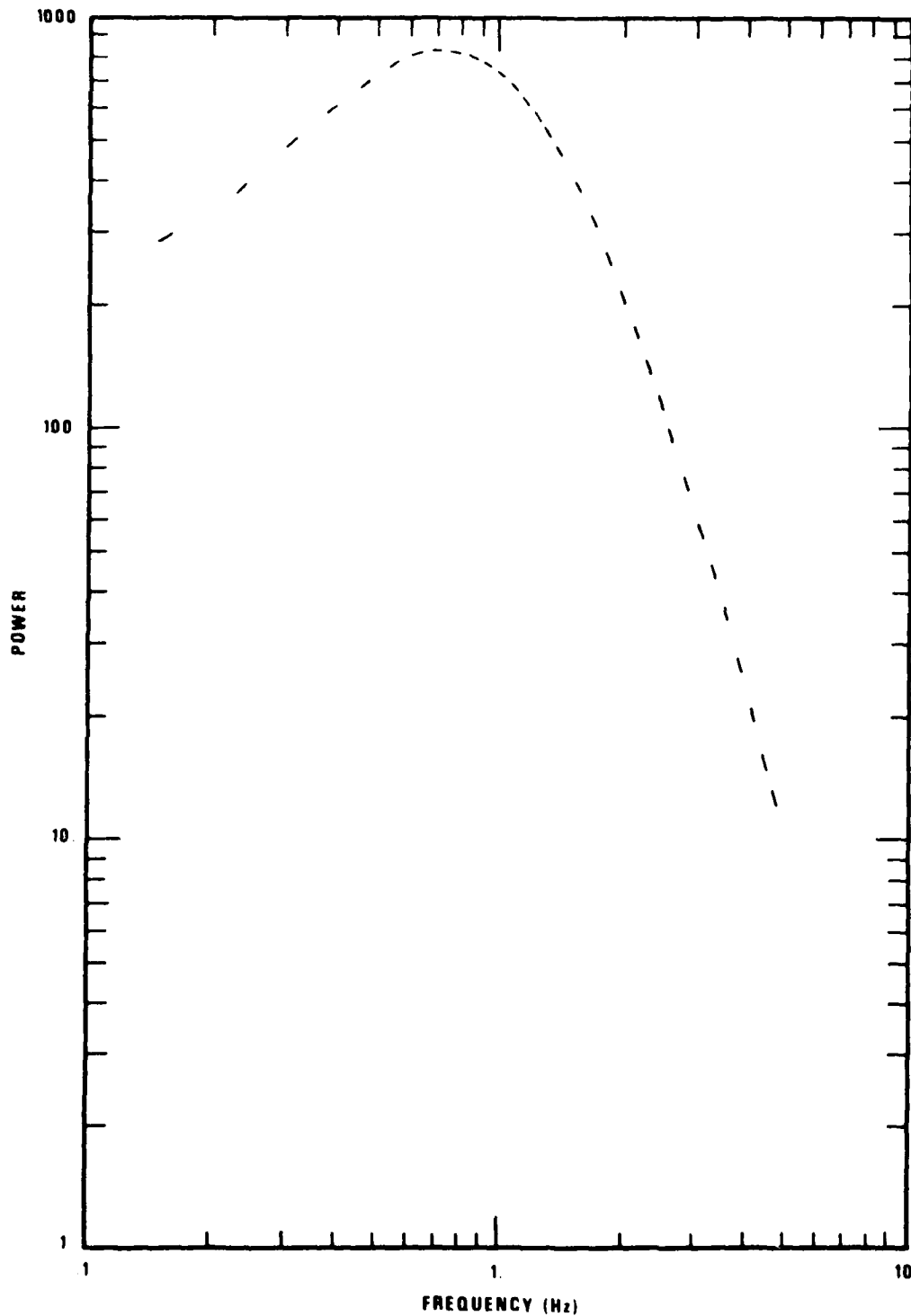


Figure 7. Source spectrum used for analysis of KNICKERBOCKER data.

# KNICKERBOCKER

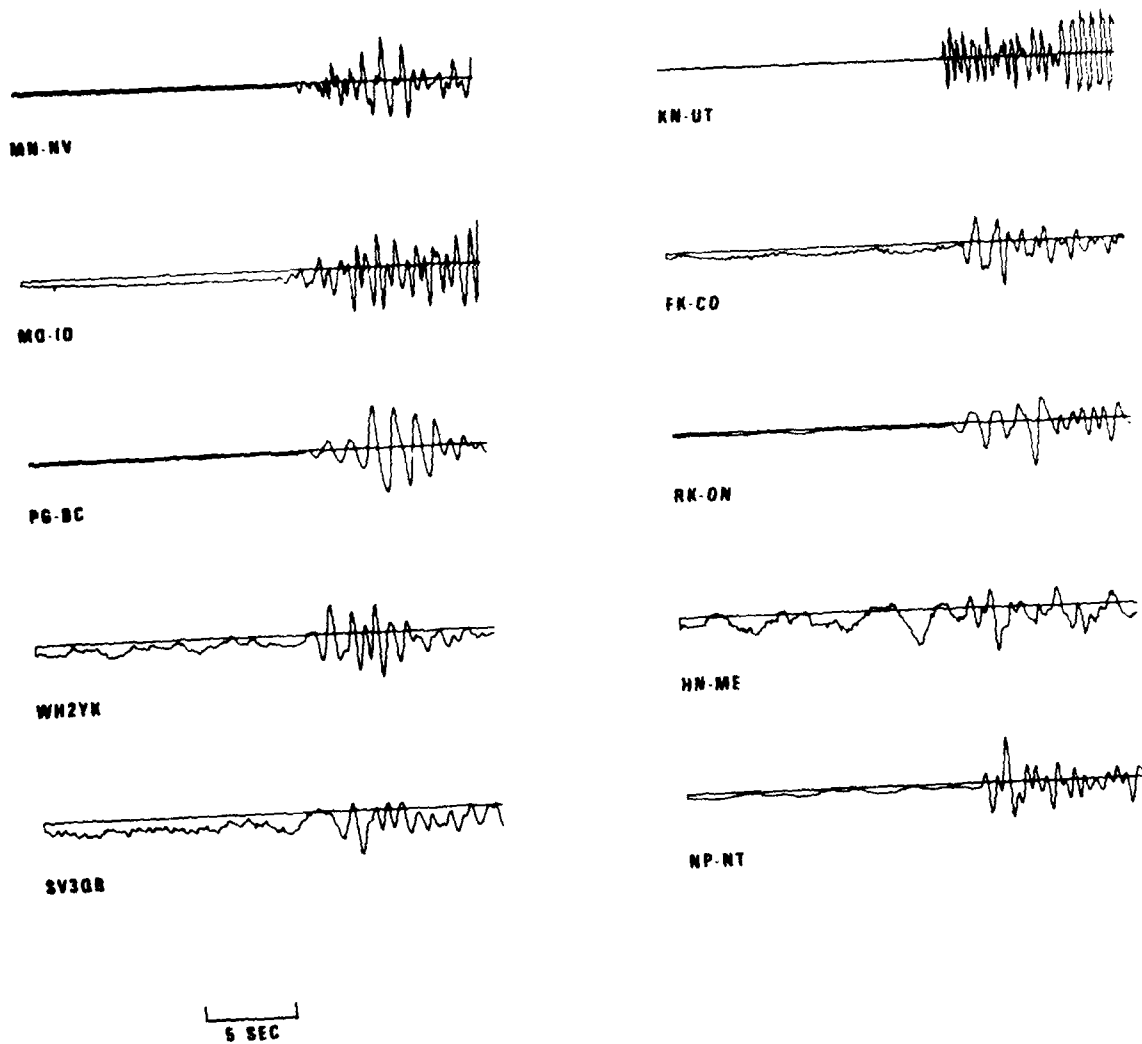


Figure 8. P-wave traces from KNICKERBOCKER.



KNICKERBOCKER

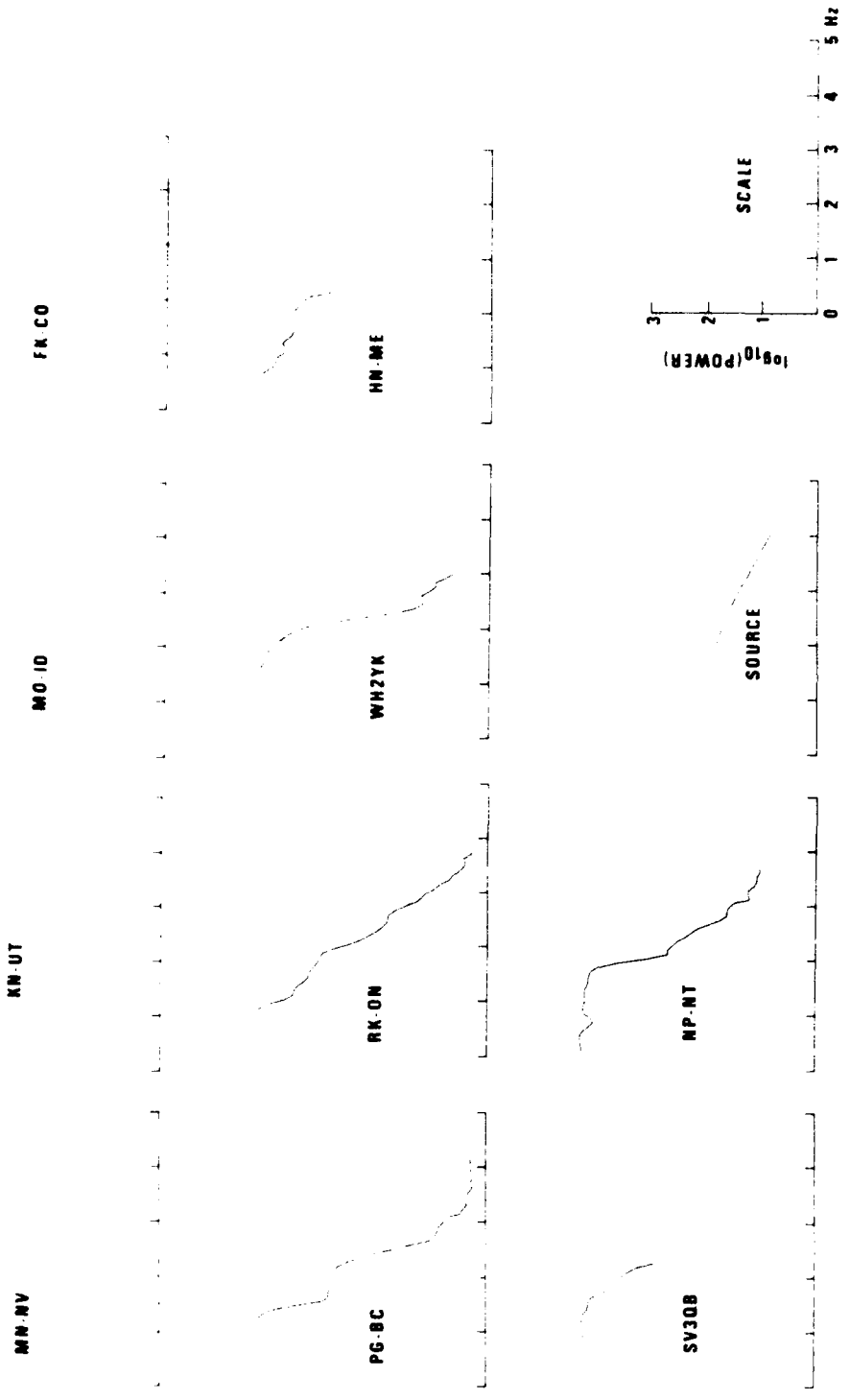


Figure 9. P-wave power spectra from KNICKERBOCKER.

KNICKERBOCKER

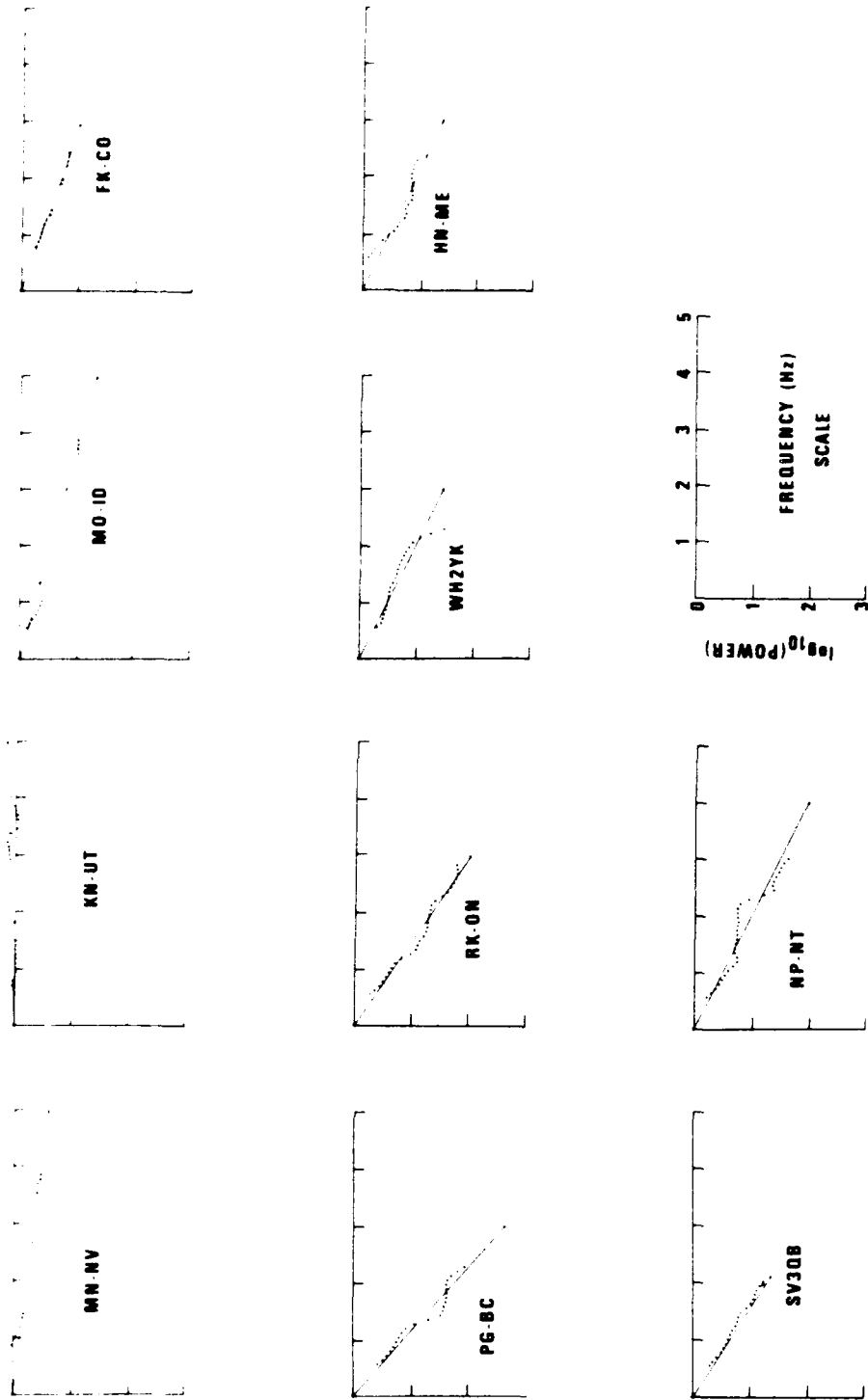


Figure 10. P-wave to source spectral ratios for KNICKERBOCKER.

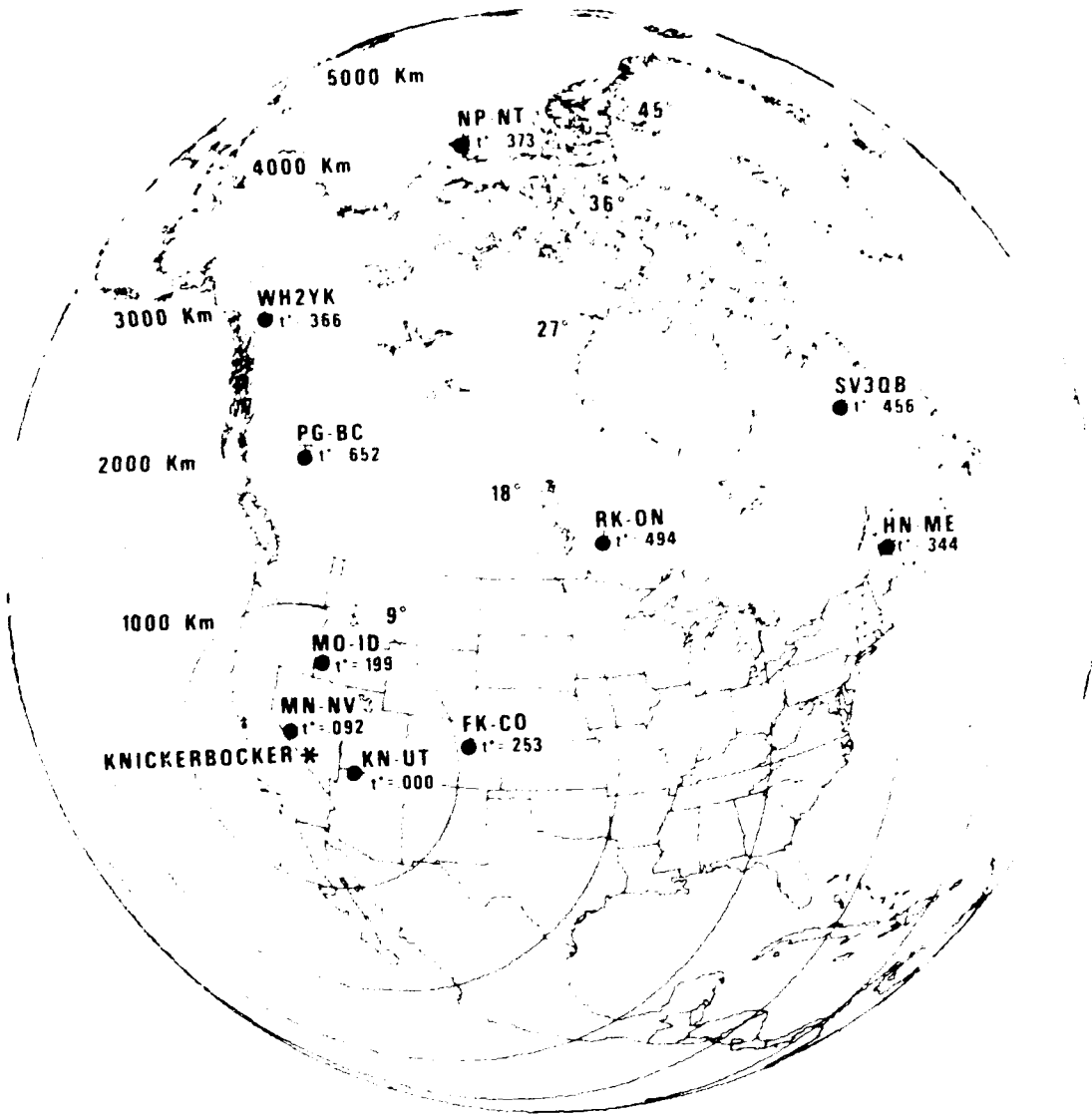


Figure 11. Location of KNICKERBOCKER and the recording stations with  $t^*$  values.

TABLE II  
 Summary of the Results of Attenuation Calculations

TABLE IIB  
 KNICKERBOCKER  
 71 kt

Station	Distance km	T Travel Time Sec	$\alpha$ Slope	Q	t*
MN-NV	197	32.34	-0.126	350	.092
KN-UT	326	48.88	+0.030	$\infty$	.000
MU-ID	647	89.76	-0.272	450	.199
FK-CO	1081	144.30	-0.345	571	.253
PG-BC	1920	243.98	-0.889	374	.652
RK-ON	2355	289.14	-0.674	585	.494
WH2YK	2917	338.17	-0.499	925	.366
HN-ME	4091	431.12	-0.469	1254	.344
SV3QB	4204	439.62	-0.622	964	.456
NP-NT	4350	450.36	-0.509	1207	.373

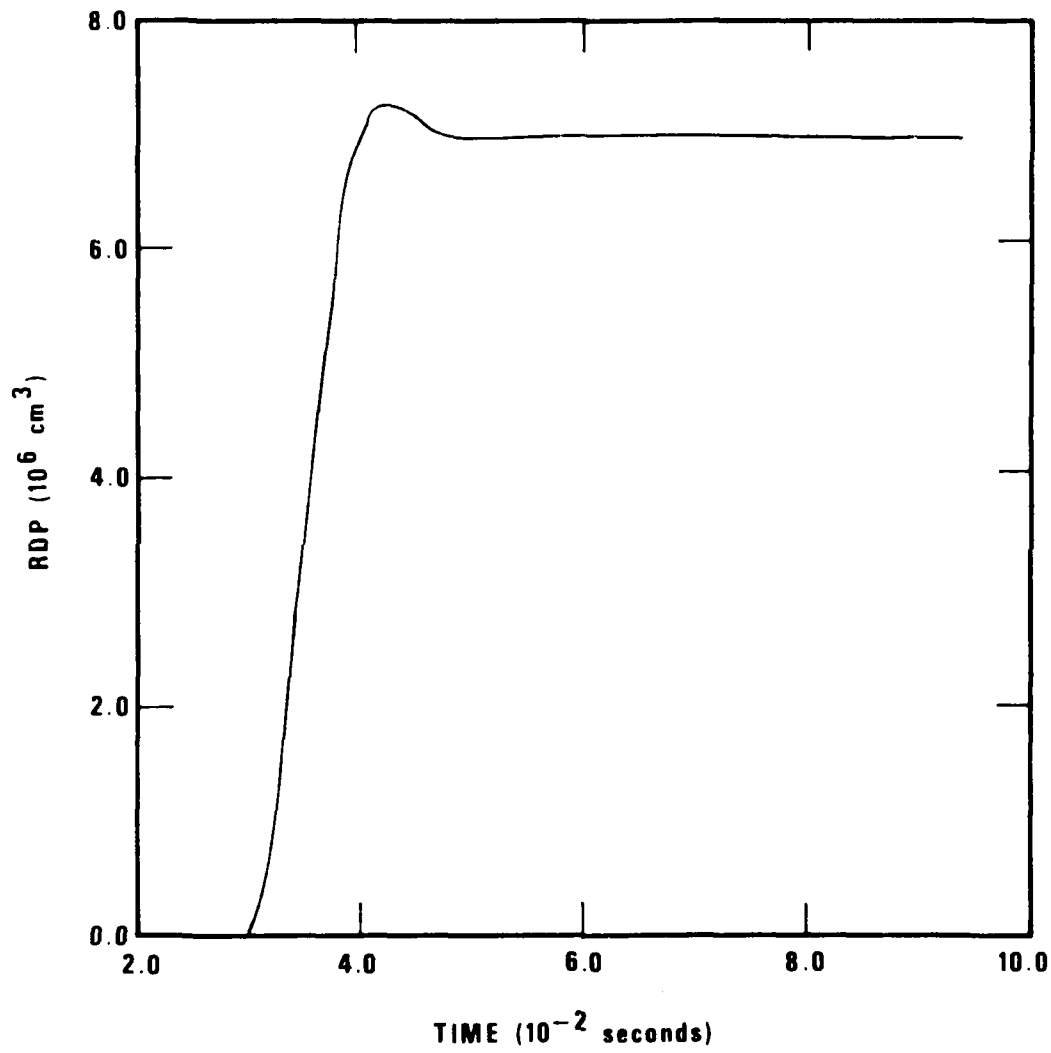


Figure 12. MAST reduced displacement potential scaled to 20 tons.

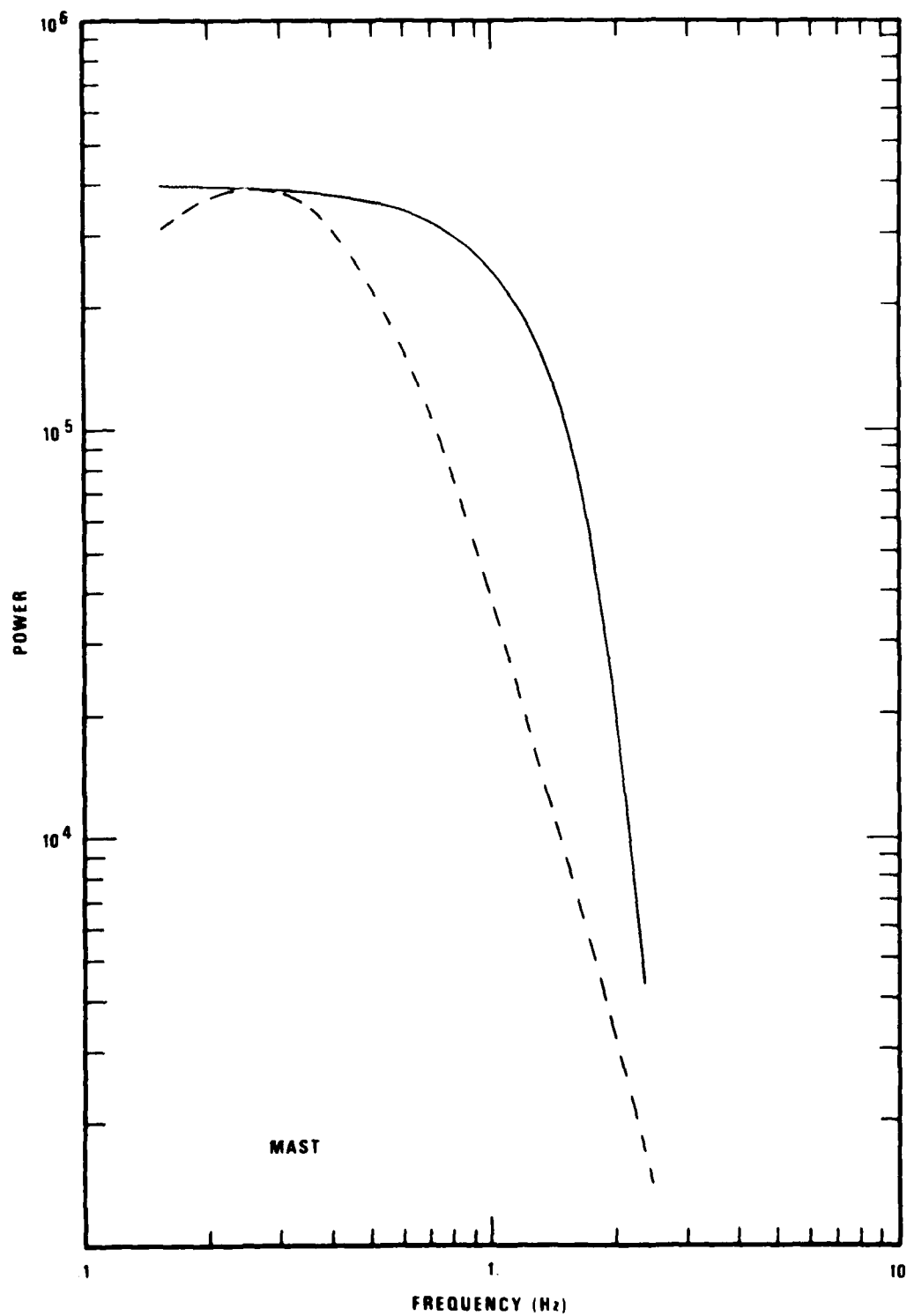
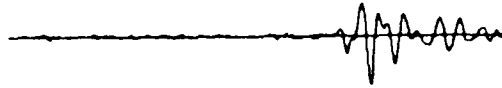


Figure 13. MAST source spectrum used in our analysis (solid line) and upscaled source spectrum of von Seggern and Blandford (1972).

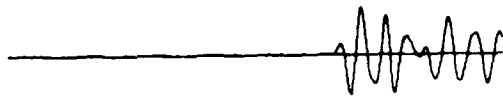
**MAST**



**RK-ON**



**CPSO**



**WHZYK**



**FN-WV**



**HN-ME**

10 sec

Figure 14. P-wave traces for MAST.

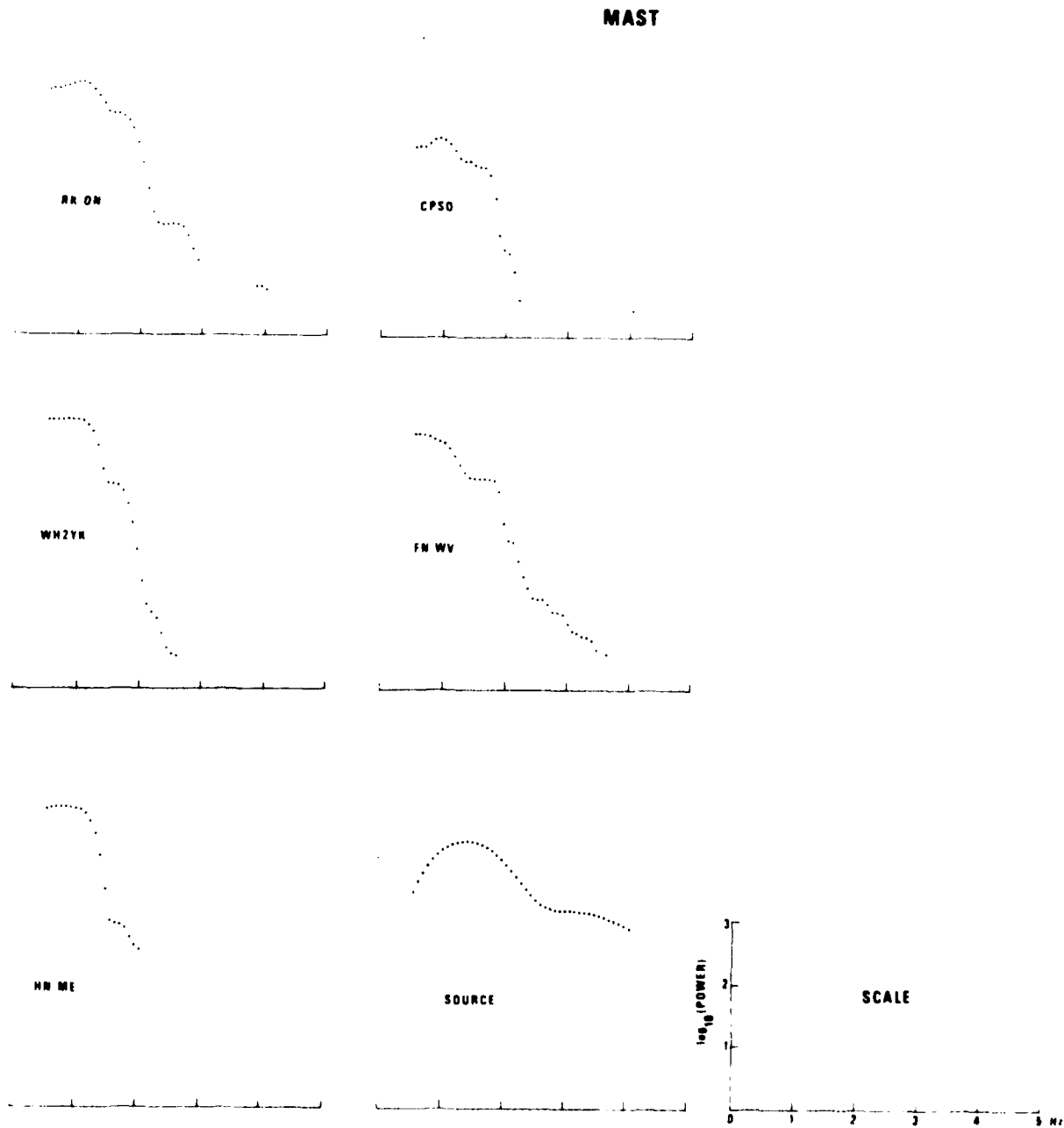


Figure 15. P-wave power spectra for MAST.



# MAST

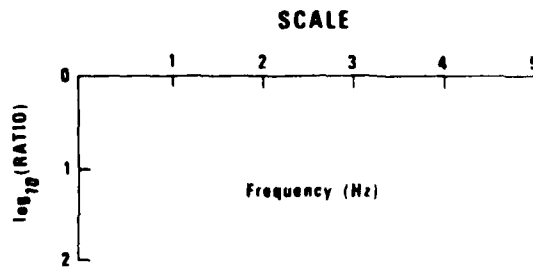
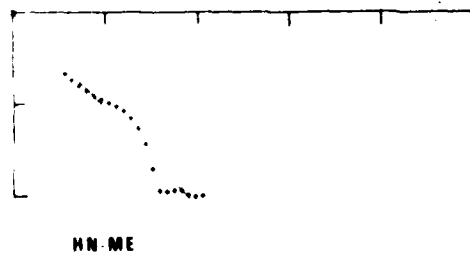
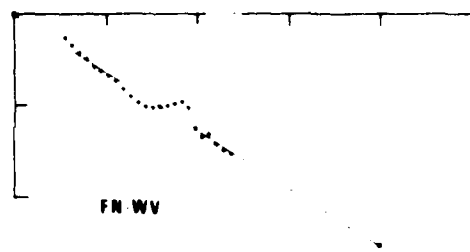
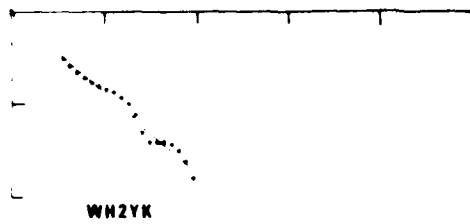
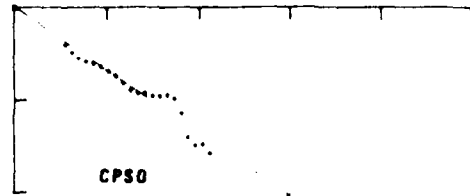
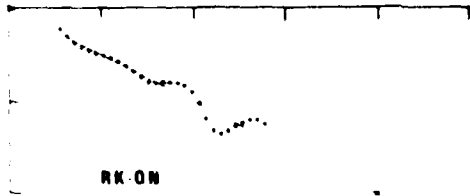


Figure 16. P-wave to source spectral ratios for MAST.

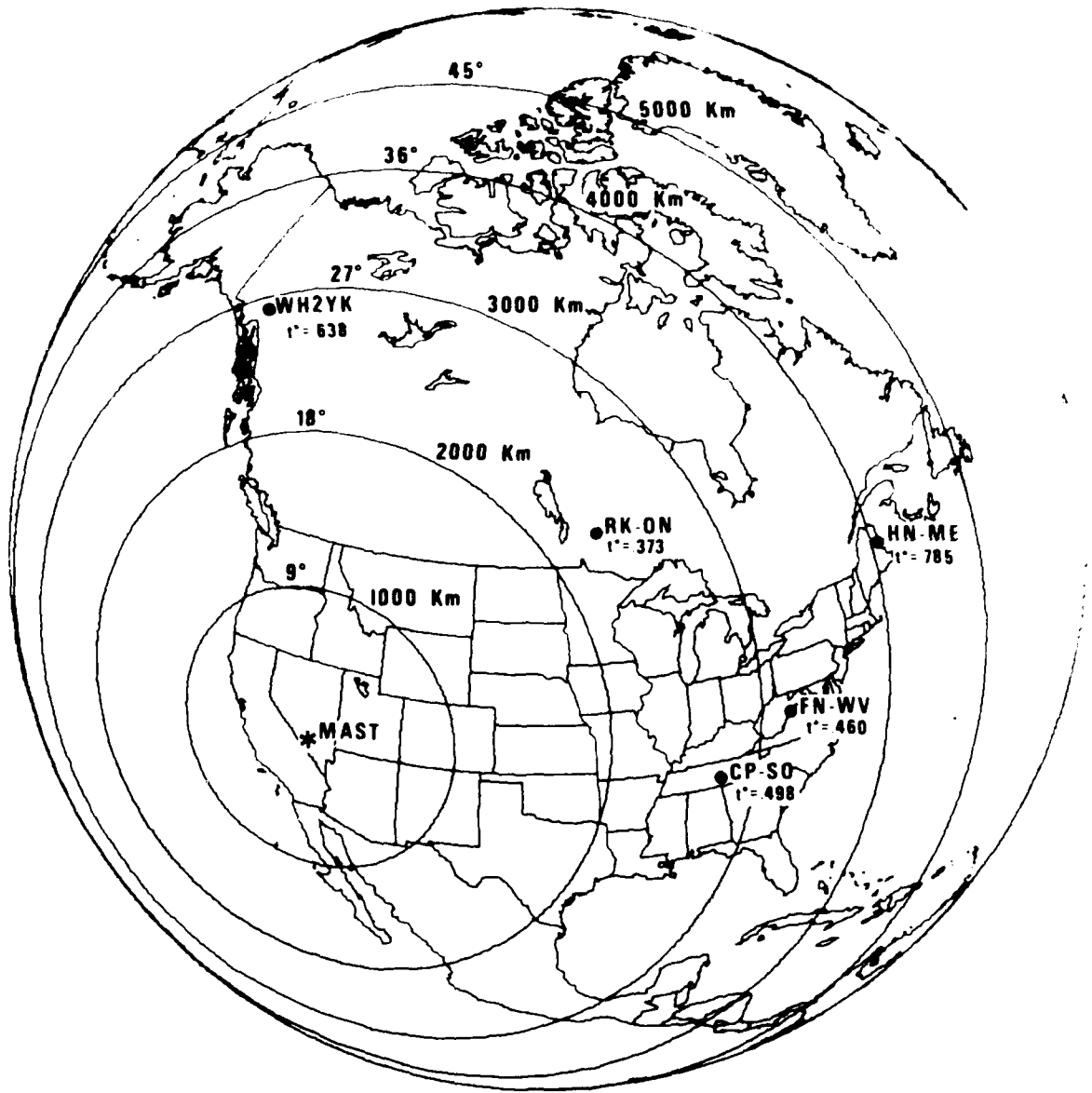


Figure 17. Location of MAST and the recording stations with  $t^*$  values.

TABLE II  
 Summary of the Results of Attenuation Calculations

TABLE IIC  
 MAST

Station	Distance km	T Travel Time Sec	$\alpha$ Slope	Q	t*
RK-ON	2335	284.5	-0.509	763	.373
CPSO	2747	321.9	-0.679	647	.498
WH2YK	2913	336.2	-0.870	527	.638
FN-WV	3214	360.5	-0.628	783	.460
HN-ME	4070	427.2	-1.071	544	.785

AEC publication (Rodean, 1971) was originally taken from Werth and Herbst (1963). Werth and Herbst used close-in measurements to derive this spectrum, shown in Figure 18. The time traces, spectra, spectral ratios are given in Figures 19, 20 and 21. The map of  $t^*$  values, stations and shot locations is given in Figure 22. Results are summarized in Table IID.

#### SALMON

This nuclear explosion was discussed extensively in a separate report (Der and McElfresh, 1975). We give only a map of locations with  $t^*$  values here, which is shown in Figure 23. We also report the  $Q$  and  $t^*$  values in Table IIE.

---

Rodean, H. C., 1971, Nuclear explosion seismology, U.S. Atomic Energy Commission, AEC Critical Review Series, Division of Technical Information.

Werth, G. C. and R. F. Herbst, 1963, Comparison of amplitudes of seismic waves from nuclear explosions in four mediums, J. Geophys. Res., v. 67, p. 1463.

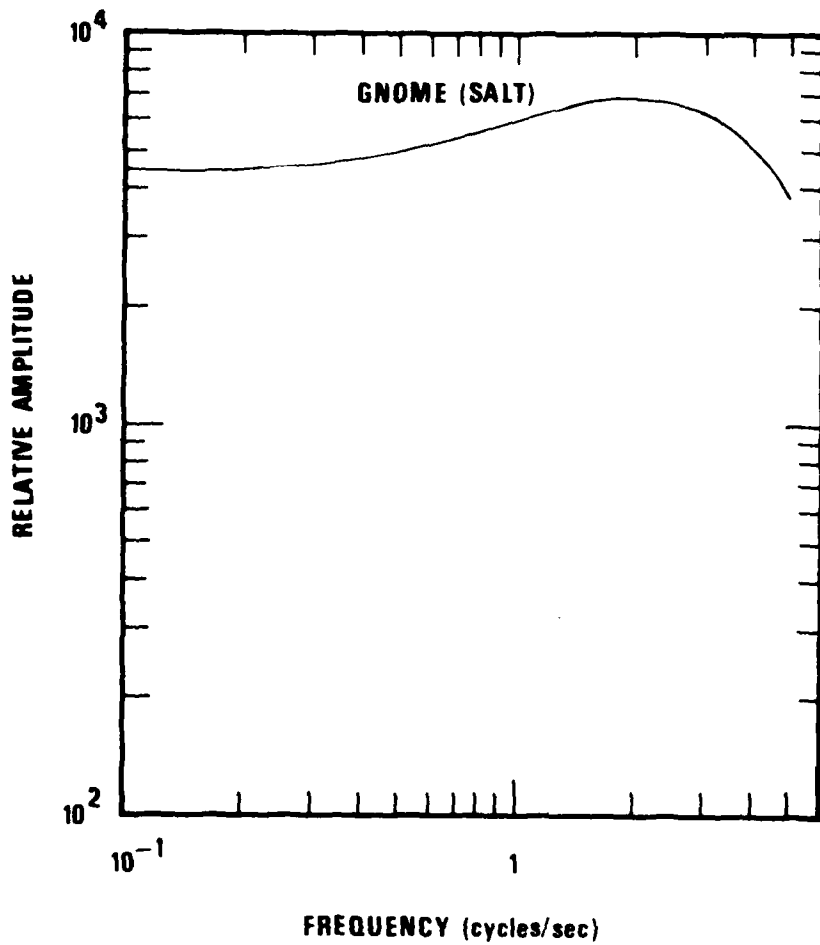


Figure 18. GNOME source spectrum.

# GNOME

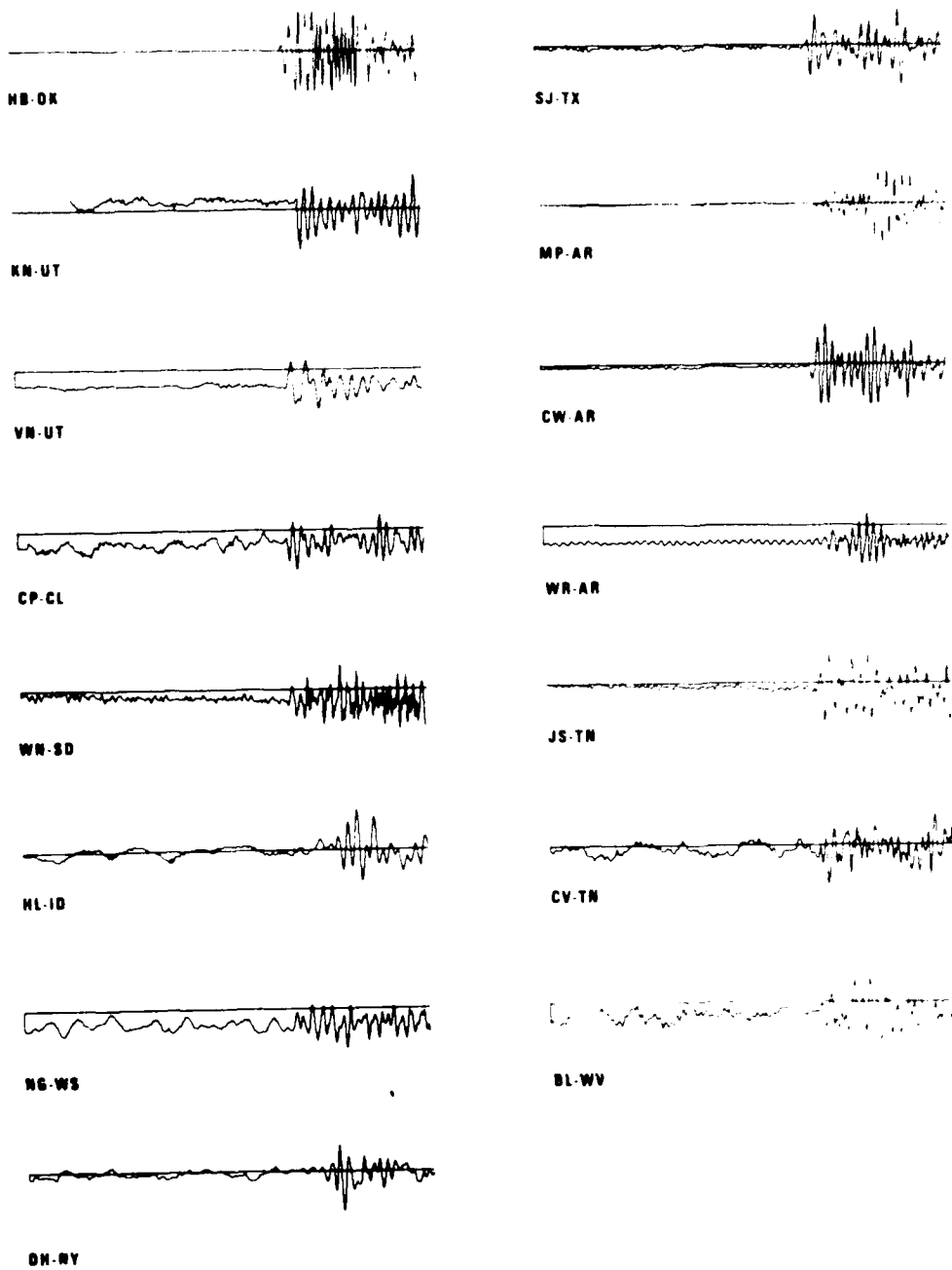


Figure 19. P-wave traces for GNOME.

GNDOME

MP AR

KN UT

SJ TX

HB OK

WR AR

CP CL

CW AR

VN UT

CV TN

HL ID

JS TN

WN SD

SOURCE

OH NY

BL WV

NG WS



Figure 20. P-wave power spectra for GNDOME.

GNOME

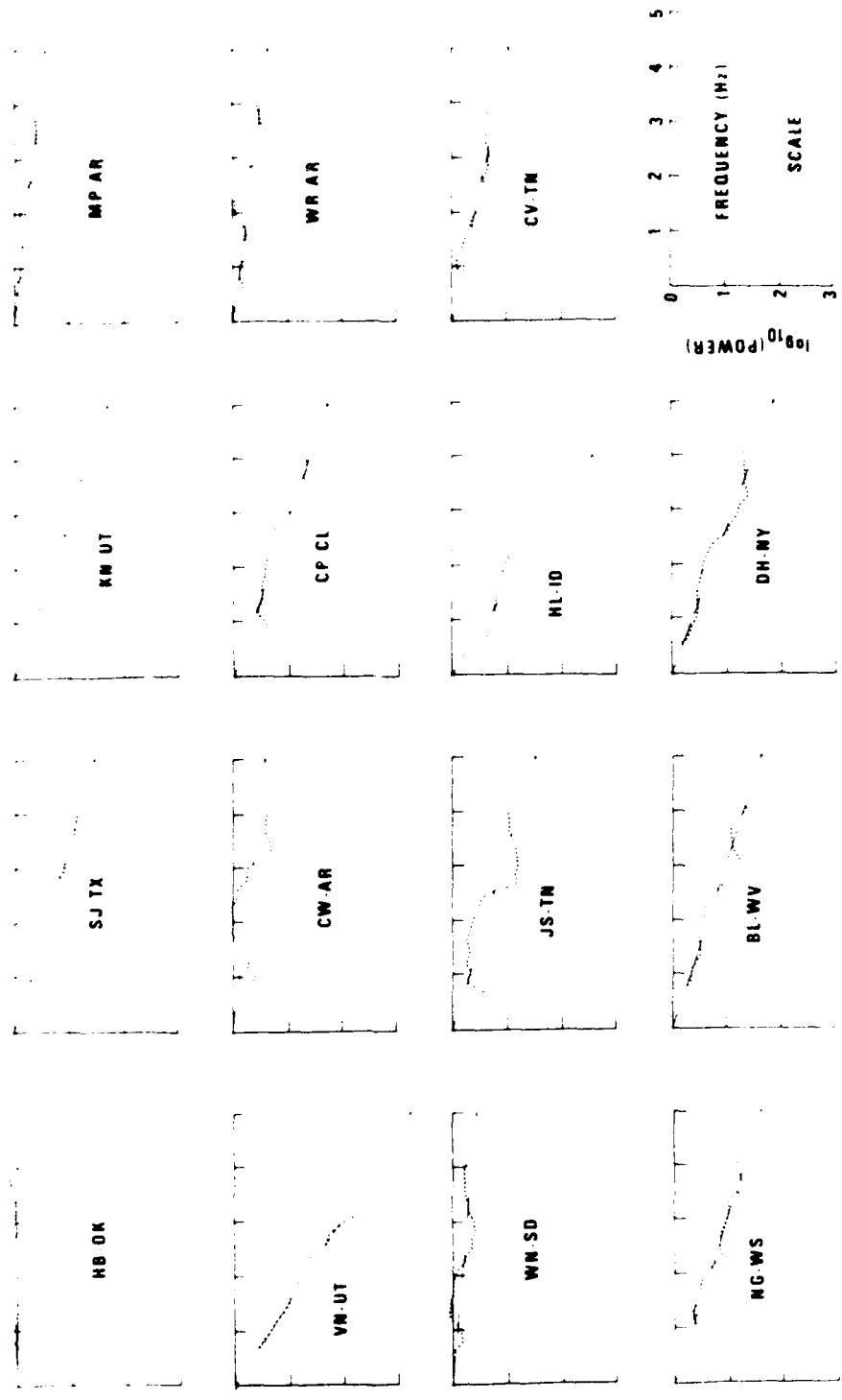


Figure 21. P-wave to source spectral ratios for GNOME.



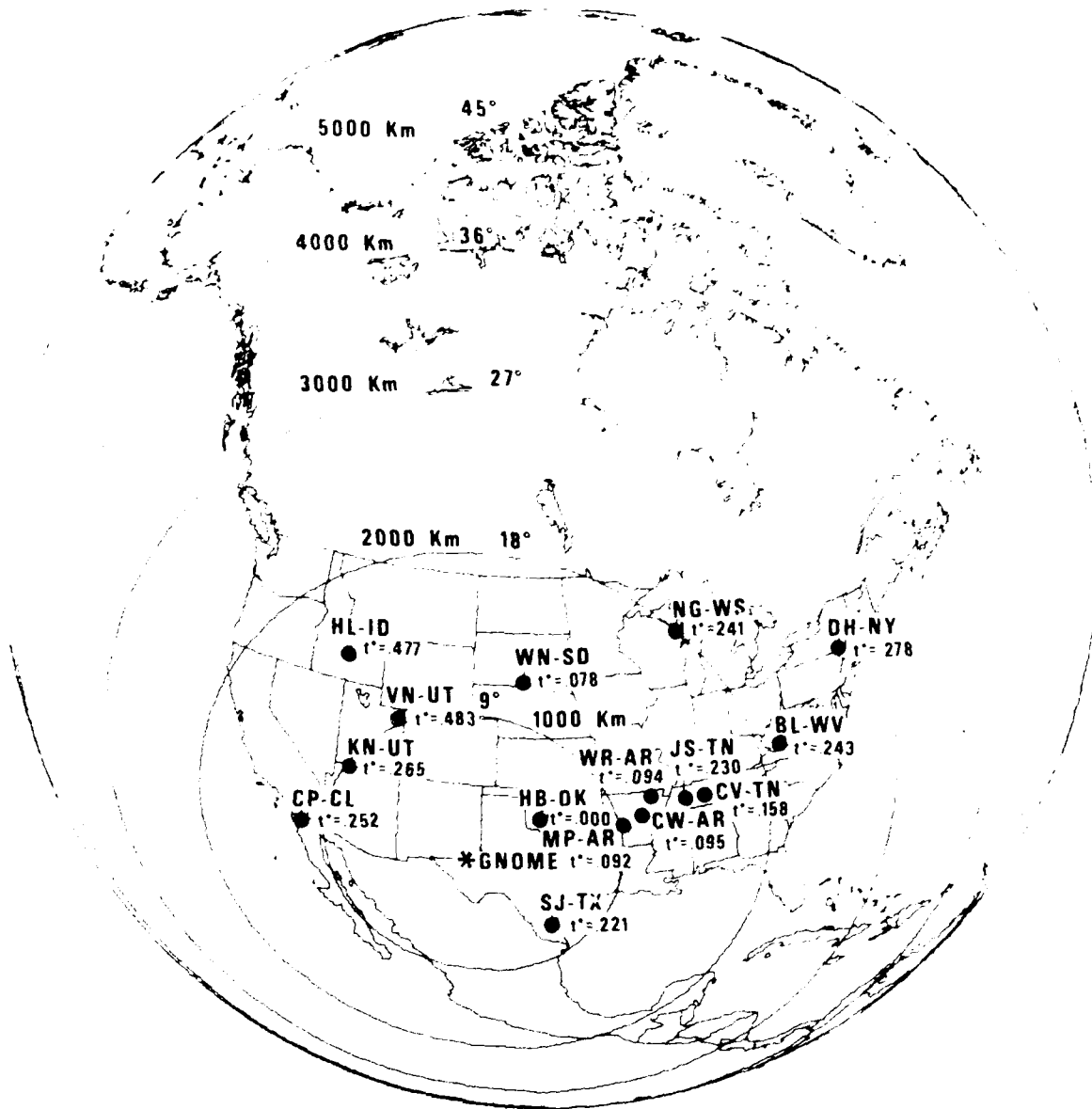


Figure 22. Location of GNOME and the recording stations with t\* values.

TABLE II  
 Summary of the Results of Attenuation Calculations

TABLE IID

GNOME

3 kt

Station	Distance km	T Travel Time Sec	$\alpha$ Slope	Q	t*
HB-OK	561.4	76.7	+0.020	$\infty$	.000
SJ-TX	743.4	99.1	-0.302	448	.221
KN-UT	975.8	127.8	-0.361	483	.265
MP-AR	1029.4	134.1	-0.126	1452	.092
KN-UT	1048.1	136.6	-0.658	283	.483
CW-AR	1146.3	148.4	-0.129	1570	.095
CP-CL	1175.5	152.1	-0.344	603	.252
WR-AR	1238.3	159.6	-0.128	1701	.094
WN-SD	1261.6	162.5	-0.106	2092	.078
JS-TN	1457.3	186.2	-0.314	809	.230
HL-ID	1556.1	198.3	-0.650	416	.477
CV-TN	1569.0	199.7	-0.215	1267	.158
NG-WS	2017.1	251.5	-0.329	1043	.241
BL-WV	2141.8	264.9	-0.331	1092	.243
DH-NY	2782.0	324.6	-0.379	1169	.278

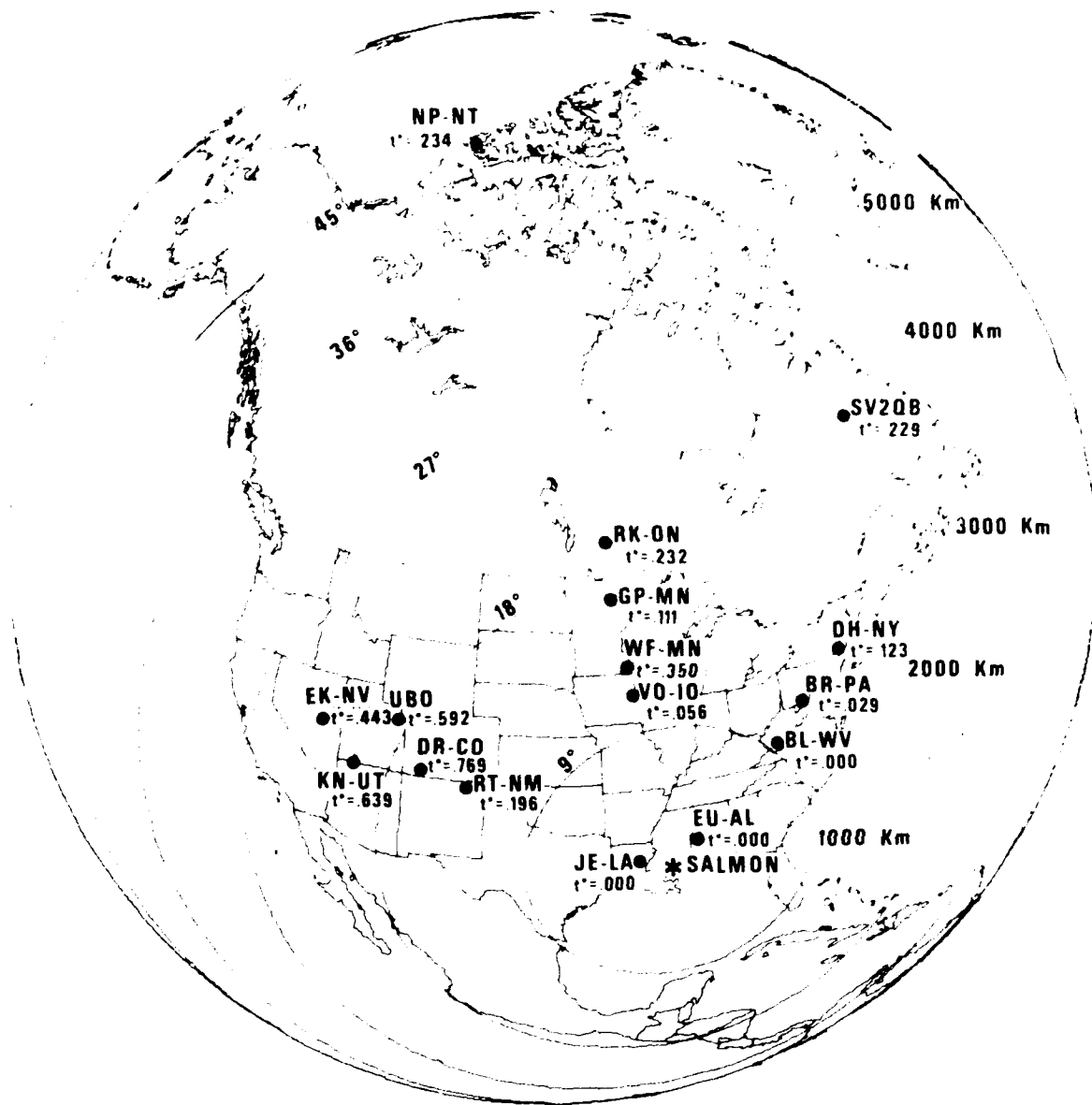


Figure 23. Location of SALMON and the recording stations with  $t^*$  values.

TABLE II  
Summary of the Results of Attenuation Calculations

TABLE IIE

SALMON

5 kt

Station	Distance km	T Travel Time Sec	$\alpha$ Slope	Q	$t^*$
EU-AL	242	36.5	0.025	$\infty$	.000
JE-LA	243	37.4	0.038	$\infty$	.000
BL-WV	1058	138.5	0.036	$\infty$	.000
VO-IO	1251	160.6	-0.076	2883	.056
BR-PA	1375	174.0	-0.039	6087	.029
WF-MN	1427	180.0	-0.477	515	.350
RT-NM	1499	190.0	-0.268	967	.196
DH-NY	1795	225.3	-0.168	1830	.123
DR-CO	1814	230.7	-1.048	300	.769
GP-MN	1865	231.4	-0.151	2091	.111
UBO	2069	260.1	-0.808	439	.592
RK-ON	2214	270.5	-0.316	1168	.232
KN-UT	2237	277.3	-0.871	434	.639
EK-NV	2533	305.4	-0.604	690	.443
SV2QB	3192	358.0	-0.312	1566	.229
NP-NT	5264	515.0	-0.319	2203	.234

## DISCUSSION

In trying to interpret the results of this study one has to keep in mind several limitations of Q determinations from P-wave spectra. At small epicentral distances ( $\Delta < 1000$  km) the Q values will be unreliable because the slopes of the spectral ratios will be just as strongly influenced by uncertainties of the source spectrum as by attenuation. Q values at greater distances will be more reliable but "discrepancies" of the order 30% should not unduly upset the reader. Variations of such magnitude are to be expected. One has to accept the fact that Q is a parameter which is very hard to determine with precision, and this is true for all attenuation studies in the literature. What we are looking for are relative changes of Q by factors of 2 or more. Occasionally one may also encounter a Q value which is "out of line" but such instances are few.

Let us discuss the general picture emerging from this study. Two of the events SALMON and GNOME show a remarkable asymmetry in the distribution of  $t^*$  and Q values with respect to azimuth. The stations located west of these shots show significantly lower Q values, while those to the east and north of the shot points show high Q values. The shots at NTS show uniformly lower Q values at all stations. At a distance of about 18-20° from the shot point the Q values are about one half of those (Q in the range 500-700) determined from SALMON for the paths in eastern North America. The Q values from GNOME seem to be somewhat lower in the east. This may be due to some attenuation under this shot point since it is located in the West close to the boundary. These Q values are slightly above 1000. We believe that it is significant that RTNM for the SALMON shot shows a Q of 967 which is very close to these values. This station is located similarly to GNOME relative to the boundary. There seems to be also a general increase of Q values at epicentral distances beyond 2000 km. We believe that the difference in Q values at NPNT between the shots at NTS (1207 for KNICKERBOCKER and 1601 for PILEDRIVER) and SALMON (2205) is also significant reflecting the lack of low Q layer under SALMON.

The features of the solutions outlined above are all consistent with the notion of a low Q layer under the western United States, while such a layer

is absent in the eastern United States. P waves from all events in the western United States will be affected by this layer. The greatest effect of this layer is in the intermediate distance range  $15^\circ < \Delta < 30^\circ$  where the effective Q value is reduced by a factor of two relative to paths not crossing this layer (Q is in the range of 400-700 instead of around 1500). In the above discussion we disregarded an anomalous measurement at WFMN for SALMON and we did not consider close-in stations ( $\Delta < 100$  km) which we regard, a priori, as unreliable. Of all the 32 measurements with  $\Delta > 1000$  only WFMN is inconsistent. The rest conform to the general pattern discussed above. The Q values at the close-in stations do not mean much, although in the case of GNOME they indicate the same azimuthal asymmetry as the rest of the measurements, but even here SJTX is anomalous.

Table II also shows the values of  $t^*$  for all measurements. The highest value is .785 (MAST to HNME), but most of the measurements along paths crossing the measured low Q layer under WUS typically give values of  $t^*$  around .45 at intermediate distances ( $1000 < \Delta < 3000$  km). At greater distances  $t^*$  for mixed EUS-WUS paths decreases somewhat, probably because the rays spend less time in the low Q layer and more time in the high-Q lower mantle. Wavepaths which are entirely under EUS show values of  $t^*$  typically less than .3. It seems, therefore, that the early estimate of the global average  $t^* \approx 1$  by Carpenter and Flinn (1965) is too high although paths under typical oceans are not considered in this study, and these may give higher  $t^*$  values. Other workers find similar  $t^*$  values (Noponen, 1975; Frasier and Filson, 1972). In estimating the effect of attenuation on P-waves travelling from NTS to the SDCS stations one can assume values of  $t^*$  in the range .4-.5.

---

Carpenter, E. W. and E. A. Flinn, 1965, Attenuation of teleseismic body waves, *Nature*, v. 207, p. 745-746.

Noponen, I., 1975, Compressional wave-power spectrum from seismic sources, Institute of Seismology, University of Helsinki, ISBN 951-45-0538-7. Contract AFOSR-72-2377 (Final Report).

Frasier, C. W. and J. Filson, 1972, A direct measurement of Earth's short-period attenuation along a teleseismic ray path, *J. Geophys. Res.*, v. 77, p. 3782-3787.

Figure 24 shows histograms of the observed  $t^*$  values presented in this paper. The  $t^*$  values for pure EUS paths (solid line) are typically below .3. Mean value is .16. The values for mixed WUS-EUS paths are greater and have a mean of .49. The shaded portion of each histogram is for measurements at  $\Delta > 4000$  km. The few  $t^*$  values we have for (possibly) pure WUS paths do not indicate  $t^*$  values significantly greater than for mixed paths (mean value .477). However, the statistical reliability of the difference is not good.

The .33 differential between the mean value of  $t^*$  for EUS and mixed EUS-WUS paths can account for about .45 magnitude units (at 1 cps) in magnitudes in the epicentral distance ranges covered in our report (mostly  $\Delta < 4000$  km). Thus a 50 kt explosion for which most of the source energy is concentrated at frequencies around 1 cps we should expect about a .45 magnitude units lower body wave magnitude if the source is located in the WUS and the paths to the stations are all the mixed type, as compared to a hypothetical explosion of the same size located in the EUS.

We do not have enough data to decide whether the .33  $t^*$  differential persists; at greater distances  $t^*$  for  $\Delta > 4000$  km seems to have a mean value (.463) not significantly different from the mean of the rest of the measurements (.497). It seems, however, from other work that such a differential persist as evidenced by teleseismic magnitude residuals (Booth, Marshall and Young, 1975). Our own work on P-wave amplitudes from selected deep focus events across the U.S. also gave differences of roughly the same magnitude between EUS and WUS (Der, Massé, and Gurski, 1975).

A smaller  $t^*$  value for EUS paths does not guarantee that magnitudes will be greater in a manner entirely consistent with  $t^*$ . It has been shown that both the velocity structure and Q structure are different in the two major subdivisions of the country, therefore the amplitude-distance dependence at close-in to intermediate distances will be different. In addition to this, multipathing and local structure also affect the amplitudes measured. In spite of this it seems that the value of  $t^*$  is a very significant factor in determining the magnitudes even at intermediate distances. Figure 25 shows a plot of GNOME and SALMON log A/T values (corrected for distances with the

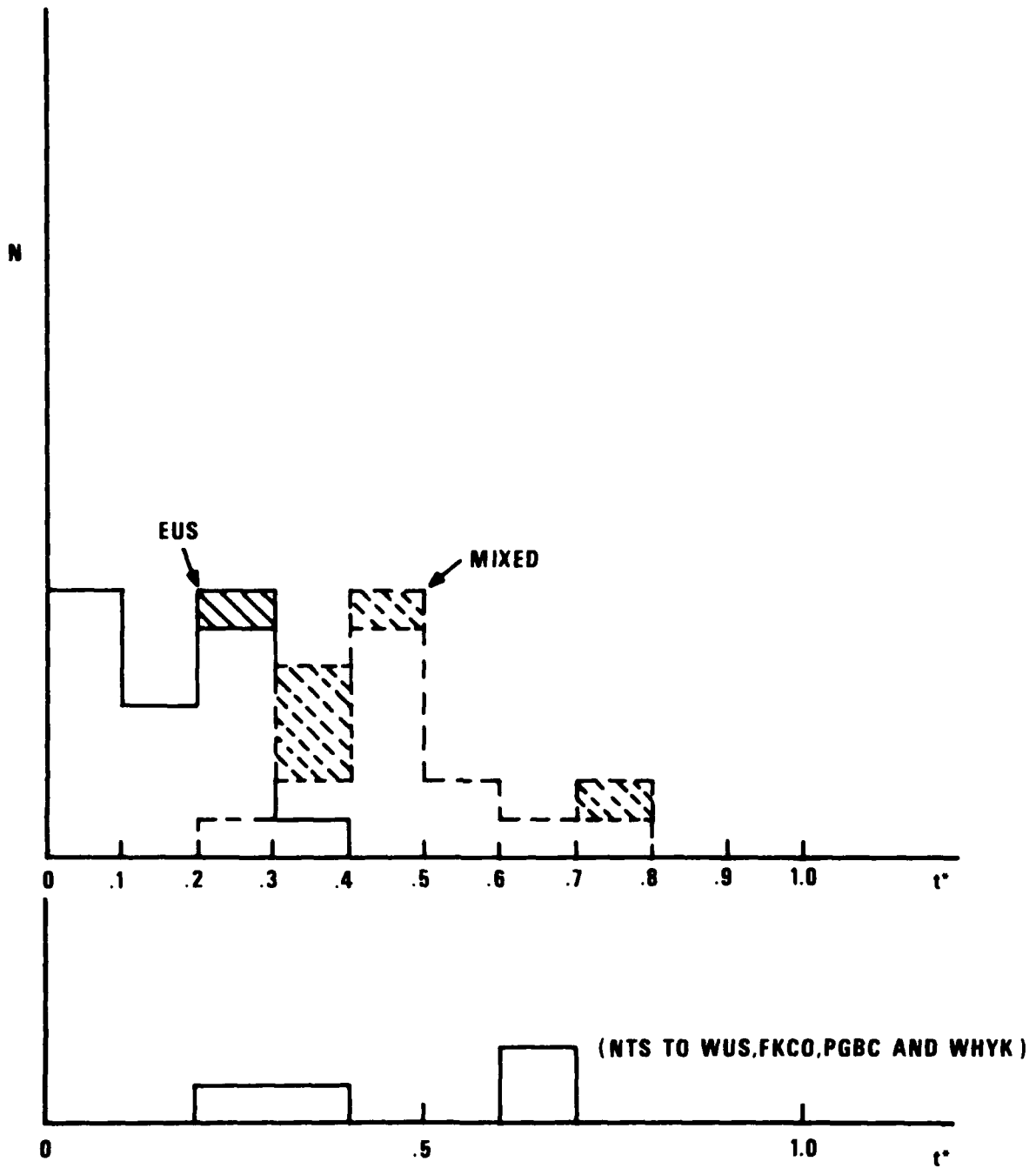


Figure 24. Histograms of all  $t^*$  measurements quoted in this paper.  
 Top: solid line - measurements for pure EUS paths  
 dashed line - measurements for mixed EUS-WUS paths  
 Bottom: possible all tectonic (WUS) type paths (NTS to WHYK, FKCO & PGBC)  
 shaded portions are for  $\Delta > 4000$  km.



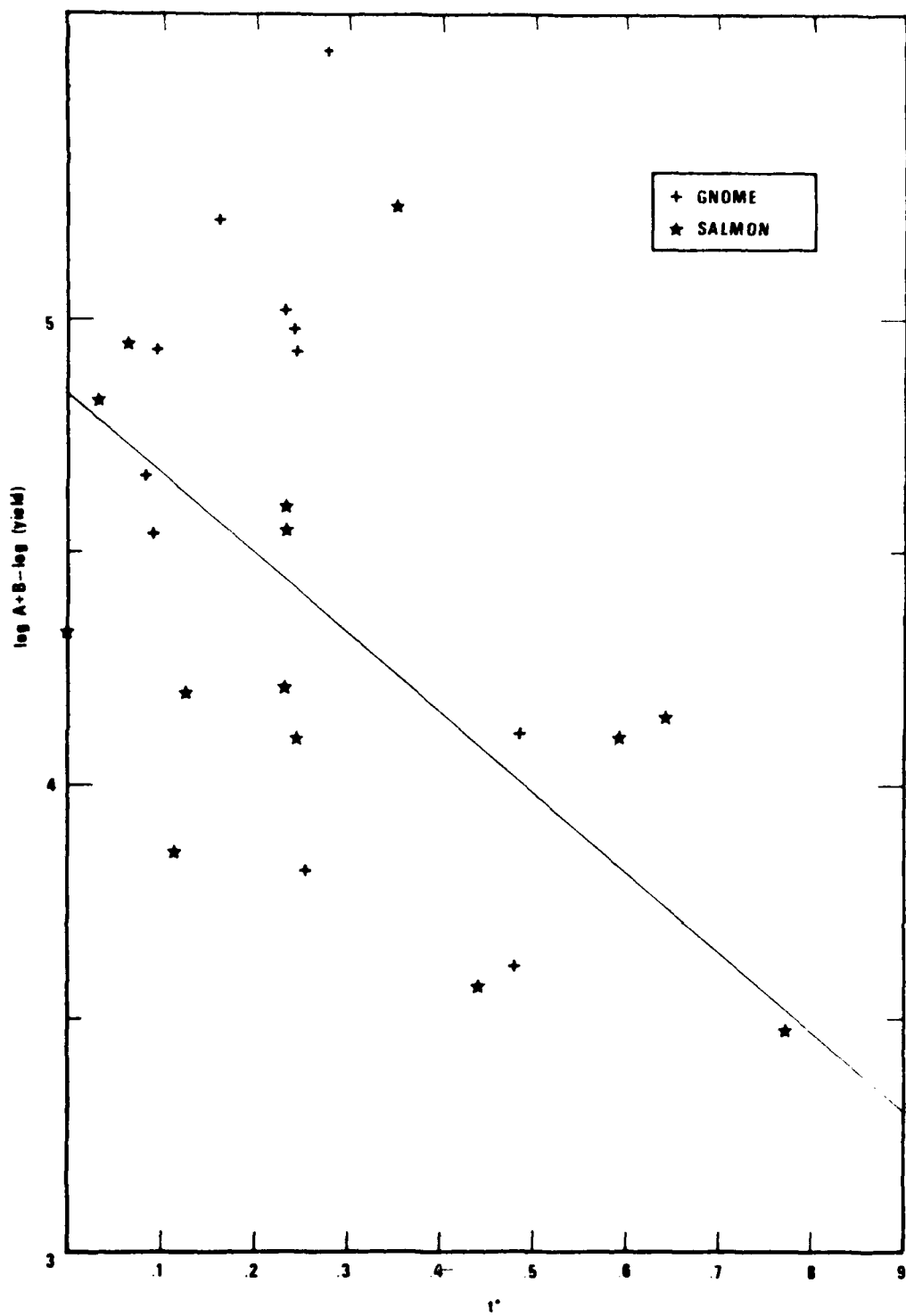


Figure 25. Plots of  $\log A/T$  (m $\mu$ /sec) vs.  $t^*$  for GNOME and SALMON. Distance (B factor) corrections have been made on  $\log (A/T)$ .

B factors of Veith and Clawson, 1972, and for the relative difference in yield). There is a considerable scatter in the measurements but the tendency of lower amplitudes to be associated with higher values of  $t^*$  is clear. Statistical analysis gave a regression coefficient of -1.28 between the corrected  $\log A/T$  and  $t^*$ , but the error limits are quite wide ( $\sigma \sim .48$ ). The line corresponding to the factor  $\exp\left(\frac{wt^*}{2}\right)$  with  $t = 1.0$  Hz has a slope of -1.36 and seems to fit the data as well as the one with slope -1.28 from the regression fit, which is not significantly different from -1.36. This slope of -1.36 would be expected if  $m_b$  were determined from the spectral amplitude at 1 Hz. Obviously the slope would be greater if  $m_b$  were determined from higher frequency spectral amplitudes. The probability that the slope is zero (that is  $t^*$  is not related to amplitude) is less than .01 based on the data shown. About 47% of the total variance of  $\log A/T$  seems to be associated with  $t^*$ . This means that a correction term related to  $t^*$  could reduce the scatter significantly. The remaining scatter is due to additional causes, some of which were quoted above.

The significant differences in attenuation along various paths precludes the use of short-period spectral discriminants without proper corrections for attenuation.

---

Veith, K. F. and G. E. Clawson, 1972, Magnitude from short period P-wave data, Bull. Seism. Soc. Am., v. 62, p. 435-452.

#### ACKNOWLEDGEMENTS

Dr. R. H. Shumway and H. Husted assisted us in some of the statistical calculations. Dr. R. R. Blandford read the report and made several useful suggestions.

#### REFERENCES

- Booth, D. C., P. D. Marshall, and J. B. Young, 1975, Long and short period amplitudes from earthquakes in the range  $0^{\circ}$ - $114^{\circ}$ , *Geophys. J. R. Astr. Soc.*, v. 39, p. 523-538.
- Carpenter, E. W. and E. A. Flinn, 1965, Attenuation of teleseismic body waves, *Nature*, v. 207, p. 745-746.
- Cherry, J. T., N. Rimer, J. M. Savino, and W. O. Wray, 1975, Improved yield determination and event identification research, *Systems, Science and Software*, SSS-R-75-2696.
- Der, Z. A., R. P. Massé, and J. P. Gurski, 1975, Regional attenuation of short-period P and S waves in the United States, *Geophys. J. R. Astr. Soc.*, v. 40, p. 85-106.
- Der, Z. A. and T. W. McElfresh, 1976, Short-period P-wave attenuation along various paths in North America as determined from P-wave spectra of the SALMON nuclear explosion, SDAC-TR-75-16, Teledyne Geotech, Alexandria, Virginia.
- Frasier, C. W. and J. Filson, 1972, A direct measurement of Earth's short-period attenuation along a teleseismic ray path, *J. Geophys. Res.*, v. 77, p. 3782-3787.
- Noponen, I., 1975, Compressional wave-power spectrum from seismic sources, Institute of Seismology, University of Helsinki, ISBN 951-45-0538-7. Contract AFOSR-72-2377 (Final Report).
- Rodean, H. C., 1971, Nuclear explosion seismology, U.S. Atomic Energy Commission, AEC Critical Review Series, Division of Technical Information.
- Veith, K. F. and G. E. Clawson, 1972, Magnitude from short period P-wave data, *Bull. Seism. Soc. Am.*, v. 62, p. 435-452.
- von Seggern, D. and R. Blandford, 1972, Source-time functions and spectra for underground nuclear explosions, *Geophys. J. R. Astr. Soc.*, v. 31, p. 83-97.
- Werth, G. C. and R. F. Herbst, 1963, Comparison of amplitudes of seismic waves from nuclear explosions in four mediums, *J. Geophys. Res.*, v. 67, p. 1463.

APPENDIX

Procedures Followed in Computing Q

## APPENDIX

### Procedures Followed in Computing Q

The short-period vertical P-wave seismograms, including a noise sample prior to the arrival of the P wave, were anti-alias filtered and digitized from magnetic tape at 20 samples/sec.

A time window comprising 9 sec of the signal and 4 sec of the preceding noise was tapered with a Parzen window and Fourier transformed, and the power spectrum was computed by multiplying the Fourier spectrum by its conjugate. This power spectrum was then smoothed by a 12-point running average. The shift of the time window was designed to avoid heavy tapering of the first arrival. A noise power spectrum ahead of this window was computed using an identical procedure and was subsequently subtracted from the spectrum of the window containing the signal.

The source spectra, determined from scaling or close-in measurements, were modified with the instrument response and also smoothed with a 12-point running average. This was done to simulate an identical treatment given to the data spectra (the effect of the Parzen window is not very significant relative to the 12-point smoothing). Instead of correcting the spectra for pP, which for any sizeable surface reflection coefficient would introduce spurious peaks into the spectrum, we rely on smoothing to eliminate any modulation present due either to pP or to other causes. The fit of straight lines to spectral ratios constitutes in effect, a final smoothing. We use only the portion of spectrum between .5 and 4 Hz, and in fitting straight lines to the spectral ratios we required that the signal power spectrum exceed that of the noise by a factor of three. Portions of spectra not satisfying this criterion are not used in the least squares fit. Furthermore, to avoid problems with the dynamic range of analog magnetic tape, the portions of power spectra which were down more than 2.5 orders of magnitude from the peak were also disregarded.

The slopes given in Table II refer to the graphs where one unit of  $\log_{10}$  (amplitude ratio) corresponds to one unit of frequency.